Université de Montréal

The role of the human INO80 complex in telomere maintenance

Par
Danielle Henry

Program of Molecular Biology, Faculty of Medicine

Mémoire présenté en vue de l'obtention du grade de Maîtrise en Biologie Moléculaire option biologie des systèmes

May 2020

Résumé

Les extrémités des chromosomes contiennent des répétitions de séquences d'ADN appelées télomères qui empêchent l'activation inopportune de la réponse aux dommages de l'ADN afin de préserver l'intégrité génomique. Les télomères raccourcissent à chaque cycle de réplication d'ADN et la télomérase a pour fonction de contrebalancer cette érosion en allongeant les télomères. Les cellules somatiques n'expriment pas la télomérase, donc leur durée de vie est normalement limitée par ce raccourcissement progressif des télomères qui conduit à l'activation de la voie p53 entraînant un arrêt de la croissance cellulaire. En revanche, les cellules cancéreuses acquièrent l'immortalité cellulaire principalement en réactivant la télomérase ou en utilisant des méthodes alternatives d'allongement des télomères basées sur la recombinaison d'ADN. Auparavant, dans notre laboratoire, un criblage CRISPR à l'échelle du génome a été réalisé dans la lignée cellulaire pré-B NALM-6 traitée avec la molécule BIBR1532, un inhibiteur de la télomérase. Ces résultats suggéraient que cinq sous-unités du complexe de remodelage de la chromatine INO80, lorsque supprimées indépendamment, réduisaient la prolifération des cellules ayant un raccourcissement des télomères induit par le BIBR1532. Mon objectif était d'étudier cette interaction génétique afin de comprendre les processus biologiques impliqués dans cette létalité synthétique. Après l'élimination des gènes codant à la fois pour la sous-unité enzymatique de la télomérase humaine (*hTERT*) ainsi que les sous-unités spécifiques du complexe INO80 humain, nous avons constaté que les cellules double-négatives avaient une capacité proliférative réduite, ce qui démontre que l'interaction génétique mesurée par criblage CRISPR est bel et bien spécifique. Étant donné le rôle du facteur de transcription p53 dans la réponse cellulaire au raccourcissement télomérique, nous avons exploré l'importance de cette voie de signalisation pour l'interaction entre le complexe INO80 humain et la télomérase. Après l'activation de p53 avec un traitement avec la molécule nutlin-3a, les niveaux d'expression de plusieurs cibles de p53 tels que *MDM2* et *CDKN1A* ont augmenté dans les cellules ayant une délétion du gène *NFRKB*, codant pour une sous-unité du complexe INO80 humain. Les cellules ayant une délétion du gène *UCHL5*, codant pour le partenaire d'interaction de *NFRKB*, ont également montré une augmentation de l'expression de *MDM2* lorsque traitées avec nutlin-3a. Enfin, la perte de télomérase (*hTERT*) modifie les niveaux d'expression des composants de la

voie p53 *CDKN1A*, *BAX* et *MDM2*. En conclusion, la suppression des gènes codant pour des sous-unités du complexe INO80 telles que *NFRKB* ou *UCHL5* est nuisible aux cellules ayant une délétion de la télomérase. Le complexe INO80 humain peut être impliqué dans l'inhibition de la voie p53, en réponse à l'activation de p53 soit par des télomères courts ou avec un traitement avec nutlin-3a. Des recherches plus approfondies sur cette interaction génétique pourraient mener au développement de nouvelles thérapies combinatoires afin d'inhiber la croissance des cellules cancéreuses.

Mot-clés: télomérase, les cellules pré-B NALM-6, le complexe INO80 humaine, *CDKN1A*, p53, létalité synthétique

Abstract

The ends of chromosomes contain telomeric repeats that prevent the DNA damage response from being activated in order to preserve genomic integrity. Telomerase functions to alleviate incomplete DNA replication at telomeres, and to repair those telomeres damaged by various means including oxidative damage. The lifespan of telomerase negative somatic cells is normally restricted by gradual telomere shortening which can lead to the activation of the p53 pathway resulting in cellular growth arrest. Cancer cells often elongate their telomeres in order to acquire cellular immortality predominantly by reactivating telomerase or by using recombination-based, alternative telomere lengthening methods. Previously in our lab, a genome-wide CRISPR screen was conducted in the pre-B cell line NALM-6 treated with a small molecule inhibitor of telomerase, BIBR1532. These previous results suggested that five subunits of the INO80 chromatin-remodeling complex, when independently deleted, reduced cellular proliferation in cells with BIBR1532 induced telomere shortening. My goal was to investigate this genetic interaction in order to understand the biological processes implicated in this synthetic lethal relationship. After the knockout of the genes encoding both the enzymatic subunit of human telomerase (*hTERT*) and specific subunits of the human INO80 complex, I found that the proliferative capacity of NALM-6 cells was reduced. This result indicates the genetic interaction identified by CRISPR screening is in fact specific. In addition, after p53 stimulation with nutlin-3a treatment, expression levels of the p53 pathway component *MDM2* were altered after the knockout of the genes encoding specific subunits of the human INO80 complex, *NFRKB* and *UCHL5*, individually. *CDKN1A* expression was also altered after nutlin-3a treatment and *NFRKB* knockout. Finally, the loss of telomerase (*hTERT*) alters the expression levels of the p53 pathway components *CDKN1A*, *BAX* and *MDM2*. In conclusion, the deletion of the genes encoding specific subunits of the INO80 complex, including *NFRKB* and *UCHL5*, is harmful to cells after *hTERT* knockout. The human INO80 complex may be involved in inhibiting the p53 pathway, in response to p53 activation by short telomeres or nutlin-3a treatment. Further investigation into this synthetic lethal relationship may shed light on new combinatorial therapeutics in cancer.

Keywords: telomerase, pre-B NALM-6 cells, the human INO80 complex, *CDKN1A*, p53, synthetic lethality

Table of Contents

List of Tables

List of Figures

Acknowledgements

I would like to thank all of the members of Harrington Lab, specifically Yahya Benslimane, for their guidance and support throughout my Master's thesis. I would also like to thank Dr. Lea Harrington for her continued positive leadership, which has allowed me to strive for an ambitious research project.

Thank you to my friends and family for their emotional support throughout the past two years.

I would also like to thank the flow cytometry platform, specifically Annie Gosselin and Angelique Bellemare-Pelletier, for their assistance with experiments throughout my project.

Abbreviations

Abbreviation	Full Name
hTERT	Human Telomerase Reverse Transcriptase
hTR	Human Telomerase RNA
ALT	Alternative Lengthening of Telomeres
PARP	Poly (ADP-ribose) Polymerase
INO80	Inositol Auxotroph 80
HDR	Homology Directed Repair
LCV2	Lenti-Clustered-Regularly-Interspaced-Short-Palindromic-Repeats-v2
LB	Luria Broth
LTR	Long Terminal Repeat
PEI	Polyethylenimine
DMEM	Dulbecco's Modified Eagle Medium
FBS	Fetal Bovine Serum
HEK	Human Embryonic Kidney
PVDF	Polyvinylidene fluoride
RPMI	Roswell Park Memorial Institute
FACS	Fluorescence-Activated Cell Sorting
GFP	Green Fluorescence Protein
KO	Knockout
PBS	Phosphate-Buffered Saline
DMSO	Dimethyl Sulfoxide
PCR	Polymerase Chain Reaction
ICE	Inference of CRISPR edits
Indels	Insertions and Deletions
MOI	Multiplicity of Infection
Penstrep	Penicillin-Streptomycin
cDNA	Complementary DNA
qPCR	Quantitative Polymerase Chain Reaction

ROS	Reactive Oxygen Species
ChIP	Chromatin Immunoprecipitation

Chapter 1 - Introduction

1.1 Telomere shortening leads to cellular senescence

Telomeres comprise the ends of chromosomes and contain short tandem sequence repeats (Muller, 1938, 1941, Blackburn, 1984). In humans, these TTAGGG repeats are home to a variety of telomeric proteins, specifically telomeric repeat factor (TRF1 and 2), causing a unique and protective structure (Morin, 1989, Bilaud *et al*., 1997, Broccoli *et al*., 1997). Due to the end replication problem, a single stranded 3' overhang is created at the end of the chromosome, allowing for the attachment of telomeric binding proteins and the formation of a T loop (Griffith *et al*., 1999). The shelterin complex is a group of proteins (TRF1, TRF2, TIN2, RAP1, POT1, TPP1) that bind to telomeres in order to block DNA damage surveillance machinery (De Lange, 2005). In addition, the shieldin complex functions to suppress end resection and promote non-homologous end joining, while the CST complex (Cdc13/Ctc1, Stn1, Ten1) binds to single stranded DNA at the telomeres to cap the ends (Gupta *et al*., 2018, Surovtseva *et al*., 2009, Miyake *et al*, 2009). Therefore, telomeres are protected from being recognized as a double strand break in order to protect coding sequences from DNA damage and repair (De Lange, 2005). If these protection mechanisms are unable to function properly, genetic disorders can arise due to telomere dysregulation (Vulliamy *et al*., 2001, Sarper *et al*., 2010, Heiss *et al*., 1998).

Without these protection mechanisms, telomeres may be recognized as double stranded breaks leading to chromosomal fusions (McClintock, 1941). Over time, telomeric repeats shorten due to the end replication problem. The end replication problem arises from incomplete replication in the 3' to 5' direction, thus resulting in a loss of nucleotides after each replicative cycle (Olovnikov, 1971, Olovnikov, 1973). After enough telomeres reach a critical length, a state of growth arrest can be triggered leading to cellular senescence (Zou *et al*., 2004). The number of cell divisions possible before the onset of growth arrest is defined as the Hayflick limit (Hayflick *et al*., 1961). The senescent state is characterized by a lack of cellular proliferation but maintained cell viability (Hayflick, 1965). Cellular senescence is a mechanism to prevent the accumulation of oncogenic mutations but can also be prematurely activated after the detection of

oncogenic stimuli (O'Brien *et al*., 1986, Dimri *et al*., 2000, Damalas *et al*., 2001, Serrano *et al*., 1997).

1.2 Cancer cells utilize telomerase upregulation to acquire cellular immortality

Some cell types have demonstrated the requirement for the rapid addition of repetitive sequences to chromosome ends during replication (Shampay *et al*., 1984). The addition of repetitive sequences was later discovered to be carried out by telomerase, and enzyme that functions to add novel telomeric repeats to the ends of chromosomes, specifically the incompletely replicated lagging strand of telomeres (Greider *et al*., 1985). Telomerase is a ribonucleoprotein complex whose catalytic core minimally consists of two components, a reverse transcriptase (*TERT*) and an RNA (*hTR*), which are sufficient for telomerase activity in cell extracts (Greider *et al*., 1985, Feng *et al*., 1995, Lingner *et al*., 1996, Nakamura *et al*., 1997, Meyerson *et al*., 1997, Harrington *et al*., 1997, Kilian *et al*., 1997, Nakayama *et al*., 1998, Tesmer *et al*., 1999, Mitchell *et al*., 2000). An H+ACA box small nucleolar complex is involved in the assembly of telomerase and the proper processing of *hTR* (Tollervey *et al*., 1997, Mitchell *et al*., 1999, Mitchell *et al*., 2000, Kiss *et al*., 2006). Telomerase functions by binding telomeric DNA, adding dNTPs to elongate the DNA strand, and finally adding GGTTAG repeats to the 3' end of the telomeric DNA (Broccoli *et al*., 1997, Chong *et al*., 1995, Baumann *et al*., 2001, Collins *et al*., 1995, Greider, 1991). Overall, the presence of telomerase in the cell is important for elongating incompletely replicated double stranded DNA at chromosome ends and to repair telomeres damaged by processes including oxidative stress (Von Zglinicki, 2002). Telomerase is not present in most cell types including somatic cells, but is expressed and active in cancer cells, germ line cells, and tumour derived cell lines (Kim *et al*., 1994, Broccoli *et al*., 1995). Thus, in somatic tissues, without the function of telomerase, telomeres shorten over time triggering cellular growth arrest (Blasco *et al*., 1997).

Telomerase is characteristically derepressed in almost all cancers cells, which can occur via spontaneous telomerase upregulation (Meyerson *et al*., 1997). Additionally, primary cells have been shown to gain immortality after exogenously enforcing *TERT* expression (Vaziri *et al*., 1998, Bodnar *et al*., 1998). Overall, it is necessary for cancer cells to maintain their telomeres in order to acquire cellular immortality and to bypass the hayflick limit. Cellular

immortality can also be acquired through a telomerase-independent mechanism, coined alternative lengthening of telomeres (ALT) (Bryan *et al*., 1995, Bryan *et al*., 1997). ALT involves homologous recombination of telomeric template DNA consequently forming a circle, identified as t-circles, leading to the rolling circle replication of telomeres (Natarajan *et al*., 2002). If cancer cells require telomere maintenance for continued proliferation, the inhibition of telomerase may be an appropriate therapeutic technique for arresting cancer cell growth.

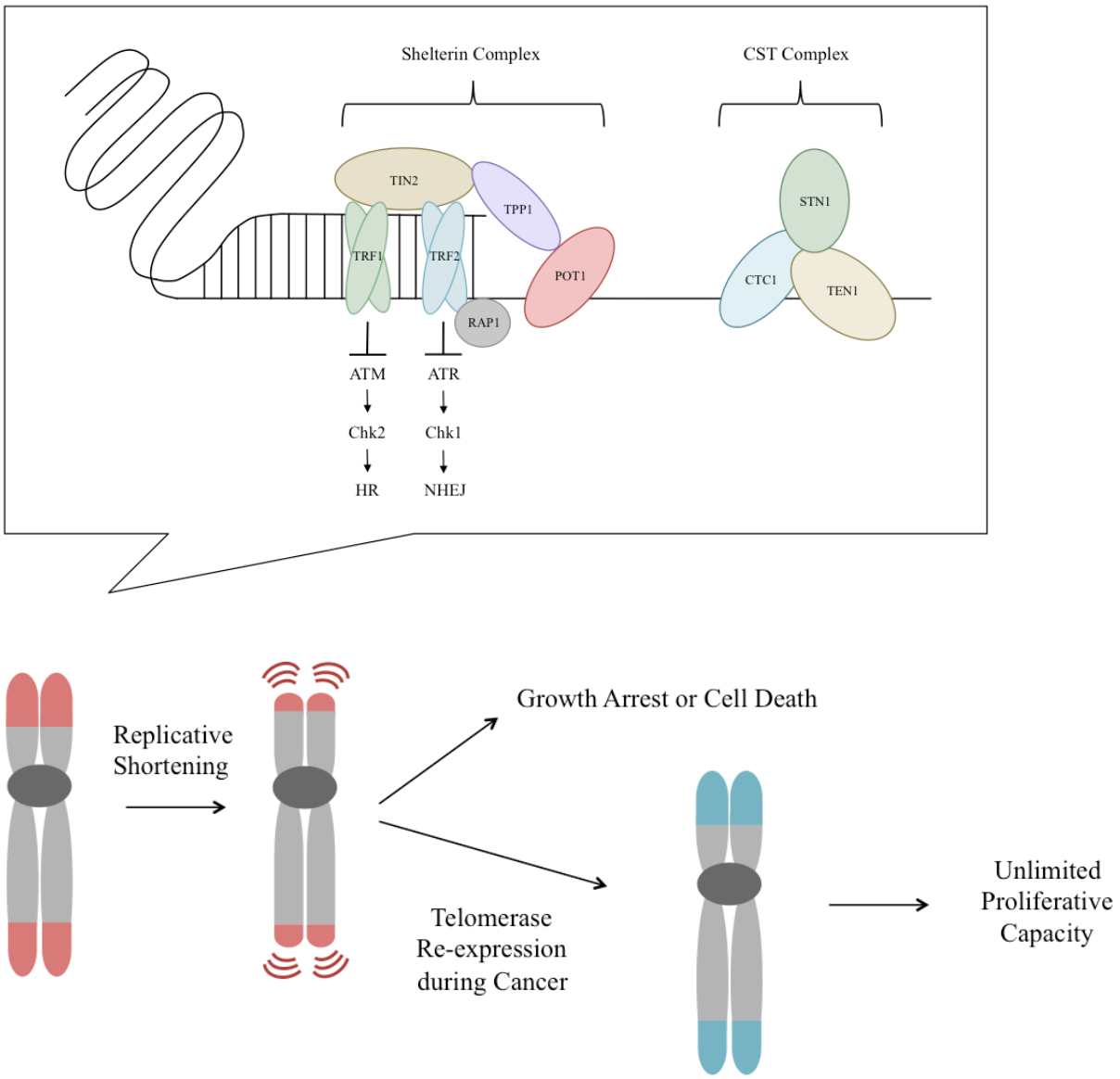

Schematic 1: Telomeric structure and alterations in different cellular contexts. Telomeres are located at the ends of chromosomes, and contain a variety of protective structures including shelterin and the CST complex. These complexes deter processes such as homologous recombination and non-homologous end joining from occurring at the single stranded telomere end. Throughout cell doublings in somatic cells, telomeres shorten due to the end replication problem. An enzyme called telomerase can use single stranded telomeric DNA as a template to elongate telomeres. Once there are enough critically short telomeres in the cell, the cell can undergo growth arrest or cell death. The cell can also re-express telomerase to maintain telomere

length in order to acquire cellular immortality, which is often the case for cancer cells. Schematic adapted from Srinivas *et al*., 2020.

1.3 The therapeutic potential of synthetic lethality with eroded telomeres

In immortalized cells with abolished telomerase activity, induced through the expression of a catalytically inactive *hTERT*, telomere shortening and decreased in vitro tumorigenic capacity ensued (Zhang *et al*., 1999, Hahn *et al*., 1999, Lundblad *et al*., 1989, Lendvay *et al*. 1996, Lingner *et al*. 1997, Nakamura *et al*., 1997). Thus, telomerase is important for the growth phenotype of malignant tumour cells (Kim *et al*. 1994, Bacchetti *et al*., 1995, Shay *et al*., 1996). TERT is an attractive target for cancer therapies, as many inhibitors have been developed. One inhibitor in particular, BIBR1532 acts as a non-nucleosidic and non-competitive inhibitor of *hTERT* and ultimately interrupts the processivity of telomerase (Pascolo *et al*., 2002). Furthermore, BIB1532 is known to bind the thumb domain of telomerase, within a hydrophobic pocket (FVYL motif) (Bryan *et al*., 2015). BIBR1532 induces a senescence-like phenotype as well as a reduction in cellular proliferation of human tumour cells (Damm *et al*., 2001, El-Daly *et al*., 2005, Pascolo *et al*., 2002). However, cellular growth arrest after telomerase inhibition requires a lag period in which telomeres must shorten. This lag period depends on the initial length of telomeres (Allsopp *et al*., 1992, Harley, 1991). Additionally, telomerase inhibitors may be ineffective due to a small proportion of tumour cells maintaining their telomeres in a telomerase-independent manner, through ALT (Bryan *et al*., 1995). Cells may also contain a mutant form of telomerase allowing for telomere maintenance in order to acquire cellular immortality, but also resistance to inhibition (Bryan *et al*., 1995). In summary, telomerase is an attractive, yet difficult target for cancer therapeutics.

Synthetic lethal relationships between genes are now being explored for their potential therapeutic use. In a synthetic lethal relationship, the altered function of one of the two proteins individually, maintains cellular growth and proliferation. However, the alteration of the two genes in the same cell results in cell death (Bridges, 1922, Dobzhansky, 1946, Lucchesi *et al*., 1968). In addition, synthetic sickness can occur if the alteration of each gene individually leads to a reduction in cell fitness, but the alteration of both genes in the same cell leads to a higher

defect in relative fitness than expected from each individual gene deletion fitness defect added together. If mutated in a particular gene, cancer cells may be addicted to, or require the function of a synthetic lethal partner for cell survival (Neckers *et al*., 2005). Thus, the inhibition of the partner leads to cell death in the mutant cancer cells only, and healthy cells maintain proliferation (Nip *et al*. 1997, Kaelin *et al*., 2004). The first drugs used in the clinic for the exploitation of synthetic lethality to kill cancer cells, include poly (ADP-ribose) polymerase (PARP) inhibitors (Farmer *et al*., 2005). The loss of the homologous recombination members breast cancer type 1 and 2 susceptibility proteins (BRCA1 and BRCA2) individually, can commonly result in the progression of breast cancer (Hall *et al*., 1990, Miki *et al*., 1994, Wooster *et al*., 1994, Wooster *et al*., 1995). In these cells, the single strand break repair protein, PARP, is highly essential for survival (Farmer *et al*., 2005). Synthetic lethal partners of telomerase could be similarly important to identify in order to accelerate cell death observed after the inhibition of telomerase in cancer cells.

1.4 The human INO80 complex functions as a chromatin remodeler

Chromatin remodeling plays many roles within the cell, including transcription, DNA repair and replication. One of the major ATP-dependent chromatin remodeling complexes is the inositol auxotroph 80 (INO80) complex. After being first discovered in yeast, this complex contains many metazoan-specific subunits and has thus evolved significantly (Ebbert *et al*., 1999, Jin *et al*., 2005). However, a set of conserved subunits were maintained (Jin *et al*., 2005). The human INO80 complex contains a core SNF2 family ATPase and helicase-SANT-associated/post-HAS (HAS/PTH) domain, actin related proteins, a GLI-Kruppel family transcription factor an N-terminus with metazoan-specific subunits, Ies proteins and AAA(+) ATPases (Chen *et al*., 2011). The conserved Snf2 ATPase catalytic domain is required for the nucleosome remodeling capabilities of the complex in yeast (Shen *et al*., 2000). The HSA/PTH domain is necessary for docking actin and actin related proteins (Szerlong *et al*., 2008). These two domains taken together, SNF2 and HSA, can reconstitute nucleosome remodeling of the human INO80 complex (Chen *et al*., 2011).

The main ATPase subunit, INO80, the metazoan-specific ubiquitin carboxyl-terminal hydrolase isozyme L5 (UCHL5) and nuclear factor related to kappaB binding protein (NFRKB) are prioritized in this thesis. UCHL5 is a deubiquitylase that plays a role in the 19S proteasome as well as the human INO80 complex. The N-terminal domain of NFRKB acts to recruit the c-terminal domain of UCHL5 to the human INO80 complex, and can inactivate deubiquitination by UCHL5 (Yao *et al*., 2008). However, reports have shown that human Rpn13 or the proteasome can activate UCHL5 in complex with the human INO80 complex (Yao *et al*., 2008).

The human INO80 complex plays a role in many cellular functions including DNA damage repair, transcription, and DNA replication etc. In order for the INO80 complex to serve these roles, the complex can exchange H2A.Z with H2A histones, slide histones as well as alter the positioning of nucleosomes at promoter regions (Papamichos-Chronakis *et al*., 2011, Udugama *et al*., 2011, Krietenstein *et al*., 2016, Brahma *et al*., 2017). The complex has been previously linked to telomere maintenance, as the loss of a functional INO80 complex induces extrachromosomal telomeric circles, telomere elongation, homology directed repair (HDR) as well as chromosome fusions (Yu *et al*., 2007, Hu *et al*., 2013).

A

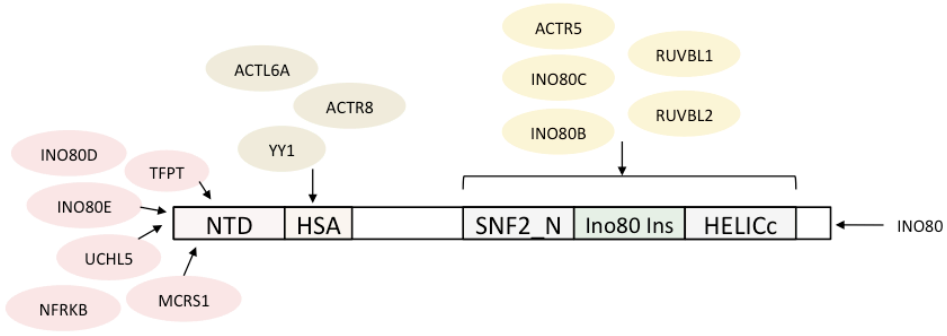

B

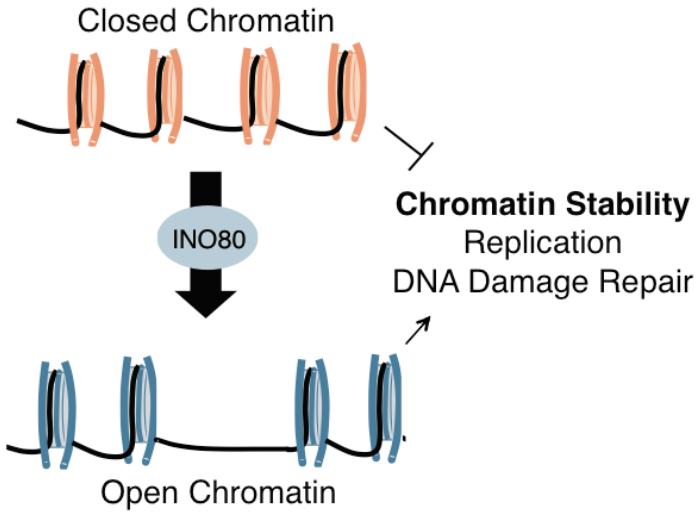

Schematic 2: The human INO80 complex contains 16 different subunits arranging into multiple domains that ultimately function in a variety of cellular processes. A) Three different complex modules assemble on different domains of INO80. The human INO80 complex contains a core SNF2 family ATPase, helicase-SANT-associated/post-HAS (HSA/PTH) domain for actin docking, and a metazoan specific N-terminal domain. The domain containing YY1AP1 has not been indicated, however, the subunit is recruited to the YY1 transcription factor subunit, and is thus a potential member of the HSA domain. **B)** The INO80 complex plays a role in many functions within the cell including chromatin stability, replication and DNA damage repair.

1.5 The role of the human INO80 complex at the p21 promoter

The human INO80 complex has also been proposed to act as a transcriptional regulator, specifically at the cyclin-dependent kinase inhibitor 1a (*CDKN1A*) promoter (Neumann *et al*., 2012, Cao *et al*., 2015). *CDKN1A* is the gene encoding $p21^{Waf1/Cip1}$ (p21). p21 acts to inhibit cyclin kinases, or regulators of cyclin-dependent kinases, thus altering cell-cycle progression (Xiong *et al*., 1993, Deng *et al*., 1995, Brugarolas *et al*., 1995). The knockdown of certain subunits of the human INO80 complex altered cell cycle regulation, specifically by delaying the progression of G2/M to G1 phase (Cao *et al*., 2015). The INO80 complex has been shown to negatively regulate p21 expression by binding to the *CDKN1A* transcriptional start site (-2.2kb and -1.0kb) only if p53 is present in the cell (Cao *et al*., 2015). These sites are also recognized as the main binding sites of p53 (El-Deiry *et al*., 1993). Thus, the INO80 complex may function to repress the transcription of *CDKN1A* in a p53 dependent manner.

1.6 The activation of the p53 pathway triggers *CDKN1A* transcriptional activation

A variety of G1 and G2 checkpoints within the cell cycle can be activated after chromosomal alterations such as DNA damage (Weinert *et al*., 1988, Hartwell *et al*., 1989). An important player in the downstream pathway of checkpoint activation is the tumour suppressor p53 (Agarwal *et al*., 1995). P53 is a transcription factor that can alter gene expression of a variety of downstream targets, including *CDKN1A* (encodes p21), which can trigger growth arrest (Bartek *et al*., 2001, reviewed in Levine, 1997). If any member of this pathway becomes aberrant, oncogenic potential is acquired (Nigro *et al*., 1989, reviewed in Abbas *et al*., 2009).

Some other key players in this pathway involve bcl-2-associated X protein (BAX), which is activated by p53 in order to induce apoptosis, and mouse double minute 2 homolog (MDM2), an E3 ligase which represses p53 activity (Toshiyuki *et al*., 1995, Miyashita *et al*., 1994, Momand *et al*., 1992). Additionally, telomere shortening has been shown to induce p53 activation, p21 activation and growth arrest (Chin *et al*., 1999, Herbig *et al*., 2004).

Overall, multiple pathways within the cell contribute to p53 activation and ultimately cellular growth arrest. If telomere shortening triggers growth arrest in a p53-mediated fashion,

and the INO80 complex can function to inhibit the transcription of *CDKN1A* in a p53 dependent manner, these two cellular pathways may be intertwined. Prior to this study it was observed that after the deletion of critical subunits of the human INO80 complex in addition to the inhibition of telomerase activity, cellular growth arrest was seen at quicker rates. For this project, it was hypothesized that the inhibition of *CDKN1A* transcription by the human INO80 complex supresses the p53 and p21 activation caused by short telomeres in order to control rates of growth arrest. This project will examine the proposed synthetic lethal relationship and the role of the human INO80 complex in telomere integrity.

Rationale

Previous reports have highlighted the impact of genome-wide CRISPR screens. RNAi and CRISPR-Cas9 screens have been used to highlight gene essentiality in a variety of cell lines, genetic backgrounds or environmental backgrounds (Cheung *et al*., 2011, Wang *et al*., 2014). Shalem *et al* used a CRISPR screen to determine which genes lead to vemurafenib (mutant melanoma cancer drug) resistance (Shalem *et al*., 2014). Synthetic lethality was first harnessed using a screening approach in order to find drug targets in cancer cells (Hartwell *et al*., 1997). Later, CRISPR screens were discovered to be an effective and high-throughput method for uncovering synthetic lethal relationships (Hart *et al*., 2015). Essentiality data is now widely available through databases including the DepMap portal from the Broad Institute, or the Biological General Repository for Interaction Datasets (BioGRID) (DepMap: available at https://depmap.org/portal/, BioGRID: Stark *et al*., 2006). Bertomeu *et al* have shown that genome-wide CRIPR-Cas9 screens can be utilized to determine the essentiality of genes in a certain genetic or environmental context (Bertomeu *et al*., 2017). Prior to my joining the Harrington laboratory, a genome-wide CRISPR-Cas9 screen was conducted in order to examine gene essentiality in a pre-B cell line (NALM-6) upon treatment with the telomerase inhibitor BIBR1532 (Y. Benslimane, T. Bortemeu, J. Coulombe-Huntington, M. Tyers, L. Harrington, unpublished). The screen identified five subunits of the human INO80 complex as putatively essential upon inhibition of telomerase by BIBR1532. These results prompted me to further investigate the synthetic lethal relationship between the loss of telomerase (*hTERT*) and the loss of critical subunits of the human INO80 complex, and to dive deeper into how this relationship informs us of cellular responses to the loss of telomere integrity. I have demonstrated a reduction in relative fitness of cells deleted for both *hTERT* and the genes encoding certain subunits of the human INO80 complex, and have proposed a potential role for p53. Further studies must be performed to unequivocally delineate the function of the human INO80 complex in allowing for cell survival after the loss of telomerase (*hTERT*).

Chapter 2 - Methods

2.1 Statistical and Data Analysis

All statistical analysis was performed on GraphPad (available at https://www.graphpad.com). Each analysis involved a one-way ANOVA with multiple comparisons, comparing all variables to a control. All IC50 determinations were predicted by GraphPad. All figures and correlation analyses were performed on R (available at https://www.r-project.org). All statistical analysis is available in Figure Supplementary Materials.

2.2 Cell Culture Conditions and Compound IC30 Determination

NALM-6 cells were maintained in Roswell Park Memorial Institute (RPMI; Wisent, 350-000-CL) media supplemented with 10% v/v FBS (Sigma, F1051-500ML). Cells were seeded at concentrations of 50 000 cells/ml if grown for 4 days, 100 000 cells/ml if grown for 3 days, 200 000 cells/ml if grown for 2 days and 400 000 cells/ml if grown for 1 day. Cells were grown at 37^{o}C, and 5% v/v CO_2. The concentration in which 30% growth inhibition of wild-type NALM-6 cells is observed is considered the IC30 of a chemical inhibitor. The IC30 of each compound was determined by performing a low-throughput proliferation assay. Wild-type NALM-6 cells (or non-targeting knockout control NALM-6 cell lines) were seeded for either 3 or 4 days at varying concentrations of compounds (concentrations listed in respective figure captions) and 0.1% v/v DMSO. Population doublings for each treatment group were then determined by finding the $\log_2$(cell density day 3 or 4/seeding density). The relative proliferation is then found by calculating the ratio of population doublings in the treatment group to population doublings in 0.1% v/v DMSO. The IC30 concentration is the treatment group in which the relative proliferation is approximately 0.7.

2.3 The creation of knockout populations of *hTERT* and each subunit of the human INO80 complex

Approximately two individual sgRNAs were designed to target an exon within each of the 16 subunits of the human INO80 complex using the GPP Web Portal available through the Broad Institute (GPP Web Portal available at https://portals.broadinstitute.org/gpp/public/analysis-tools/sgrna-design). The guide sequences are listed in Supplementary Figure S1. These guides were then cloned in to the LentiCRISPRv2 (LCV2) backbone using the protocol made available by the Zhang Lab (Sanjana *et al*., 2014, Shalem *et al*., 2014).

The following changes were made to the Zhang Lab protocol; the backbone was digested with *BsmB*I using an incubation time of 90 minutes (*BsmBI*; Thermo Scientific, ER0451). The product was gel extracted using the EZ10 Spin Column DNA Gel Extraction kit (BioBasic, BS654) with the following changes; the entire product was loaded into the column, three washes were performed, the empty column was spun for 2 minutes to remove excess ethanol, and the plasmid was eluted in 50 µl ddH_2O then adjusted to 25 ng/µl in ddH_2O. The ligation product was transformed into MachOne or Stbl3 competent cells (ThermoFisher, Mach1: C82003, Stbl3: C737303). Colonies were grown on plates of Luria Broth (LB) media supplemented with 100 µg/ml Ampicillin and a single colony was amplified in 5 ml of LB media supplemented with 100 µg/ml Ampicillin and incubated overnight (LB; Invitrogen, 12780052, Ampicillin; Gibco, 11593027). The plasmids were then purified using a miniprep kit (BioBasic BS614) and eluted in 50 µl ddH_2O. The plasmids were diluted to 200 ng/µl and sequenced using the LCV2-sequencing primer (Supplementary Figure S1) to confirm the insertion of the guide RNA.

In order to generate lentivirus for each of the guides contained within the LCV2-eGFP plasmid, the following components were mixed; 6 µg psPAX2, 3 µg VSVg, 9 µg long-terminal-repeat-bearing (LTR-bearing) plasmid and ddH_2O up to a total volume of 666 µl (reagents and protocols as described in Sanjana *et al*. 2014, Shalem *et al*., 2014).

Fifty-three µL of polyethylenimine (PEI) (1 mg/µl) were added and the reaction was incubated at room temperature for 15 minutes (PEI: Sigma, P3143). Each reaction was added to 10 ml Dulbecco's Modified Eagle Medium (DMEM) (Invitrogen, 11995-065) supplemented with 10% v/v Fetal Bovine Serum (FBS) and added to a 10 cm dish that is 80-90% sa/sa

confluent with human embryonic kidney (HEK) 293T cells (ATCC CRL-3216). The cells were incubated at 37^{o} C for 16 hours. The media was then replaced with 10 ml DMEM supplemented with 2% v/v FBS. The cells were incubated at 37^{o} C for 32 hours. The media was then filtered through a 0.45 μM Polyvinylidene fluoride (PVDF) filter and sucrose, $MgCl_2$ and HEPES were added to a final concentration of 5% w/v, 2 mM and 10 mM respectively (PVDF filter: Sigma, HVLP04700, sucrose: Sigma, S0389, $MgCl_2$: Sigma, 208337, HEPES: Sigma, H3375).

NALM-6 cells were maintained in RPMI media supplemented with 10% v/v FBS. RPMI media was supplemented with 10 μg/ml protamine sulfate and varying volumes of lentivirus previously generated for each guide RNA until a final volume of 1 ml was reached (Sigma, P3369). Thus, multiple reactions were created for each guide RNA. The reaction was incubated at room temperature for 15 minutes, and 1 million NALM-6 cells were added to the reaction bringing the total volume to 2 ml. The cells were incubated at 37^{o}C, and 5% v/v CO_2 for 2 days. The cells were then brought to fluorescence-activated cell sorting (FACS) to determine the proportion of the population expressing green fluorescence protein (GFP). The population giving approximately 50% GFP positive cells was chosen for each guide RNA, and all other reactions were discarded. This time point was referred to as day 0 throughout CRISPR knockout experiments.

2.4 Relative fitness determination of knockout populations

Each knockout (KO) population was followed over 12 days after day 0 (14 days post transduction) in order to determine the proportion of GFP positive cells in the population over time. Every three days, two cell pellets were collected (approximately 250 000 cells) from each population. One pellet was used to prepare genomic DNA (followed methods indicated in Truett *et al*. 2000, changes to protocol include adding only 50 μl of each buffer to the pellet, and 10 minute incubation, *TERT* locus PCR genomic DNA extraction was done using PrepGEM (MicroGEM; PUN0050)) and the other pellet was resuspended in phosphate-buffered saline (PBS) and analyzed by FACs in order to determine the proportion of GFP positive cells in the population (PBS: Wisent; 311-425-CL) (Truett *et al*., 2000). The knockout cell populations were maintained at 100 000 cells/ml and diluted every three days. The cell densities were recorded after every three days of growth. Cellular proliferation of each population was defined as the

ratio of cumulative population doublings in a specific compound or cellular background divided by that in dimethyl sulfoxide (DMSO) (DMSO; Sigma, D2650).

Relative fitness was defined as:

X = % GFP positive cells (value in decimal form)

Y =$LOG_2(X/(100-X))$

Overall Slope = (Slope of Y) / (slope of time points in days)

Population Doublings = LOG_2((Cell Density Day y + 3) / Cell Density day y)

Cumulative Population Doublings (CPD) = Sum of Population Doublings for entire timespan of experiment

Relative Proliferation = $CPD_{compound}$/ CPD_{DMSO}

Gko = (Overall Slope / Relative Proliferation) + 1.25

Relative Fitness = $Gko_{compound}/Gko_{DMSO}$

Relative fitness and proliferation calculations are provided in figure supplementary materials. Two primers were designed to target each gene of interest and are located approximately 250 base pairs away from the two guide RNAs designed to target that gene (Supplementary Figure S1, S2). The polymerase chain reaction (PCR) product would thus include both guide RNA target sites inside. The genomic DNA prepared from each time point after knockout, and for each knock out cell line, was then used as a PCR template with the previously mentioned primers (PCR methods and conditions: Supplementary Figure S2). This PCR protocol was also carried out with wild type NALM-6 cell genomic DNA as a control. KAPA high fidelity DNA polymerase (HiFi) was used for each locus PCR reaction, and changes made to the protocol are indicated in Supplementary Figure S2 (Roche; KK2501). A 5X CES PCR enhancer solution was added to some PCR reactions (indicated in Supplementary Figure S2), which is composed of 2.7 M Betaine, 6.7 mM Dithiothreitol (DTT), 6.7% DMSO v/v and 55 μg/ml Bovine Serum Albumin (BSA) (Betaine: Sigma; B0300, DTT: Sigma; GE17-1318-01, BSA: Sigma; A2153). The PCR products were then sequenced using sanger sequencing with the indicated sequencing primer (Supplementary Figure S1). The ab1 sequencing files for the knockout cell lines and wild type control were loaded onto Inference of CRISPR edits (ICE) synthego online bioinformatic tool in order to determine the percentage of insertions and deletions (indels) in each knockout population compared to the control (ICE synthego available at: https://www.ice.synthego.com). The indel efficiency of each guide RNA was determined by

the ratio of the ICE score to the percentage of GFP positive cells at that same time point (day 6 or 12). All calculated indel efficiencies are described in Supplementary Figure S3.

2.5 Competitive growth assay with BIBR1532

Compounds were purchased as a powder and dissolved in DMSO to their stock concentration. After each knockout population was maintained in culture for 12 days (14 days post transduction), each population was seeded at a density of 100 000 cells/ml in RPMI media supplemented with 10% v/v FBS and 1 μM BIBR1532 to a total volume of 2 ml (BIBR1532; Selleckchem, S1186). Prior to the start of this study (Benslimane, Y *et al*., unpublished), the 30% inhibitory concentration (IC30) of BIBR1532 was determined to be 1 μM, or the concentration at which there is a 30% inhibition of proliferation of wild type NALM-6 cells compared to wildtype NALM-6 cells grown in 0.1% v/v DMSO. A stock concentration of 1000X was prepared by diluting the compound in DMSO, in order to have a maximum concentration of 0.1% v/v DMSO. Each population was also seeded at the same cell density in 0.1% v/v DMSO. Each population was counted, brought to FACs to analyze the proportion of GFP positive cells in the population and diluted in their respective compound every three days. Relative fitness was determined for each knockout cell line in BIBR1532 compared to DMSO over 18 days.

2.6 Clonal selection for the deletion of telomerase and subunits of the human INO80 complex

NALM-6 cells were transduced with LCV2-Puromycin with a guide targeting *TERT* (Supplementary Figure S1) following the same transduction protocol as mentioned above, but also including a non-transduced control (LentiCRISPR-V2-Puro: Addgene 52961) (Sanjana *et al*., 2014, Shalem *et al*., 2014). 4 days after transduction, the population was seeded at 200 000 cells/ml in RPMI media supplemented with 10% v/v FBS and 1 μg/ml puromycin (Thermo Fisher, A1113802) and maintained for approximately 5 days until the non-transduced control cells were dead. The transduction condition that yielded a multiplicity of infection (MOI) of 0.3-0.5 was chosen to move forward with clonal selection by dilution. A cell pellet of 250 000 cells

was then collected in order to prepare genomic DNA with prepGEM and to quantify indels in the telomerase gene (PrepGEM: ZyGEM^{TM}, VWR catalog number 76218-662) using the methods described above. The cell population was then diluted to 62.5 K cells/ml and four subsequent serial dilutions by a factor of 10. The cells are then at 6.25 cells/ml in a total volume of 20 ml. 20 ml of filtered conditioned media was added and 800 µl of 100X penicillin-streptomycin (Penstrep: Sigma P4333). 200 µl of this mixture was dispensed into each well of a 96 well plate. Growth was monitored and each clonal population was amplified over time. A cell pellet from each population was taken to prepare genomic DNA using prepGEM, and indels were quantified using the TERT amplification primers (Supplementary Figure S1, S2). Each clone was genotyped as described in Supplementary Figure S4. Cellular proliferation was calculated as described above for each of the TERT knock out clones (Figure 4).

INO80 KO clones were generated using scarless nucleofection of the LCV2-EGFP plasmids containing each of the previously mentioned guide RNAs into NALM-6 cells (Supplementary Figure S1). 2 µg of each plasmid were added to 1 million NALM-6 cells individually which were resuspended in 100 µl PBS. The nucleofection protocol CV-104 was used (nucleofection protocol available at: https://www.knowledge.lonza.com/cell?id=812) and the cells were seeded in 2 ml RPMI media supplemented with 10% v/v FBS. The cells were incubated at 37^{o}C, 5% v/v CO_2 overnight. Conditioned RPMI media was filtered using a 0.22 µM filter and mixed 1:1 with fresh RPMI. Penstrep was added to a 1X final concentration. The cells were brought to FACs in PBS, and sorted for single GFP positive cells in 100 µl of the combination media in each well of a 96 well plate. The plates were incubated at 37^{o}C and amplified over time. Indels were quantified (Supplementary Figure S3) and the genotypes of each clone is listed in Supplementary Figure S4.

2.7 Changes made for the competitive growth assay with UCHL5 inhibitors

The relative fitness values of telomerase knockout populations were determined over six days with the treatment of the two UCHL5 inhibitors, NSC-687852 and WP-1130, at the IC30 concentrations of 0.02 µM and 1 µM respectively (NSC-687852: Cedarlane, 4566/10, WP-1130: Cedarlane ABX076791-5MG).

2.8 The deletion of both telomerase and each subunit of the human INO80 complex

INO80 knockout populations were created in the telomerase knockout clone 2 and in non-targeting control clonal backgrounds (D11 clone, LCV2-puromycin background, was kindly provided by Benslimane, Y. unpublished) (Supplementary Figure S1) following the same transduction protocol as above. The telomerase knockout clone 2 was transduced with guide RNAs targeting the INO80 complex at 29 days old. The relative fitness of each population was determined by comparing the growth patterns of each cell line to the clone background transduced with a non-targeting control guide RNA. Relative fitness was determined from day 3 until day 24.

Relative Fitness Calculations over Day 3-24:

X = % GFP positive cells (value in decimal form)

$Y = LOG_2(X/(100-X))$

Overall Slope (Day 3-24) = (Slope of Y) / (slope of time points in days)

Relative Proliferation was then found only for cells deleted for D11 (Non-targeting control) in either an *hTERT* KO or D11 KO clonal background.

Population Doublings = LOG_2((Cell Density Day y + 3) / Cell Density day y)

Cumulative Population Doublings (CPD) = Sum of Population Doublings for entire timespan of experiment

Relative Proliferation = $CPD_{\text{of cell line}}$/ 21

Gko = Overall Slope + Relative Proliferation $_{\text{of clonal background cell line}}$

Relative Fitness = $Gko/Gko_{\text{Conal background + Non-targeting control KO}}$

Exact calculations are provided in Figure Supplementary Materials.

Instantaneous Relative Fitness Calculations

The only alteration to the above calculations include determining the slope for each 2 or 3 day interval, and normalizing the growth rate as indicated below.

Gko = Overall Slope + Relative Proliferation $_{\text{of clonal background cell line}}$

Normalized $Gko = Gko/Gko_{\text{Conal background + Non-targeting control KO}}$

Relative Fitness = Normalized $Gko_{\text{x KO}}$/Normalized $Gko_{\text{Non-targeting Clonal Background + X KO}}$

Exact calculations are provided in Figure Supplementary Materials.

2.9 Treating cells deleted for telomerase with nutlin-3a, NSC-687852 and WP-1130

Telomerase knockout populations (age: 16 days post transduction) were sorted to collect 800 000 GFP positive cells. Non-targeting knockout populations were also sorted as a control. The cells were amplified and maintained for 7 days at 37^{o}C, 5% v/v CO_2. After 23 days (labeled Day 0 of compound treatment) post transduction, a cell pellet of 1 million cells was collected for each cell line for RNA extraction. Each cell line was seeded at 100 000 cells/ml every 3 days at the IC30 concentration of either nutlin-3a (2 μM, as determined by Benslimane, Y *et al*. unpublished), NSC-687852 (0.02 μM), WP-1130 (1 μM) or 0.1% v/v DMSO and maintained for 6 days (nutlin-3a; Sigma SML0580). After day 6 of compound treatment, another 1 million cell pellet was collected from each treatment of each cell line in order to extract RNA.

2.10 RNA extraction and qPCR

RNA was extracted from each cell pellet using the RNeasy kit (Qiagen, 217004: changes to protocol: on column DNase treatment and corresponding DNase treatment steps were removed). 0.5 μg of RNA was then synthesized into complementary DNA (cDNA) using the Superscript IV firststrand kit with random hexamer primers (Thermo Fisher, 18091050). The resulting cDNA was diluted 1:4 with ddH_2O. Quantitative PCR (qPCR) primers (Supplementary Figure S1) were designed to target *CDKN1A*, *BAX* and *MDM2*. Each primer combination was added to the PowerUP SYBR mastermix (ThermoFisher, A25776). *GAPDH* and *HPRT* primers were used as housekeeping genes for amplification controls (Supplementary Figure S1). Each pellet collected for Day 0 and Day 6 was analyzed by qPCR using primers designed for *CDKN1A*, *BAX*, *MDM2*, *GAPDH* and *HPRT*. The following program was used: 50^{o}C for 2 minutes, 95^{o}C for 2 minutes, 40 cycles of 95^{o}C for 1 second and 60^{o}C for 30 seconds. Analysis methods are described in Vandesompele *et al*., 2002 using a non-targeting control cell line as the reference sample.

2.11 Treating cells deleted for INO80 subunits with nutlin-3a for 4 hours to determine changes in p53 target expression

INO80 subunit knockout clones (Supplementary Figure S4) and non-targeting knockout clones were treated at an IC30 of 2 μM of nutlin-3a, an inhibitor of *MDM2* and thus an activator of p53, or 0.1% v/v DMSO as a control. The cells were incubated at 37^{o}C for 4 hours. One-million cells were pelleted for each treatment and cell line. RNA extraction, cDNA preparation and qPCR followed as mentioned above.

2.12 IC50 proliferation assay of cells deleted for subunits of the INO80 complex treated with nutlin-3a and doxorubicin

INO80 subunit knockout clones (Supplementary Figure S4) and non-targeting knockout clones were treated with varying concentrations of nutlin-3a (0.5 μM, 1 μM, 2 μM, 4 μM) and doxorubicin (1.25 nM, 2.5 nM, 5 nM, 10 nM, 20 nM) and 0.1% v/v DMSO (doxorubicin; Sigma, D1515). The cells were seeded at 50 000 cells/ml with the aforementioned compounds and incubated at 37^{o}C, 5% v/v CO_2 for 4 days. Cell densities were determined after 4 days in order to determine the relative proliferation of each combination of INO80 subunit knockout clone and compound concentration. Relative proliferation was determined as mentioned above. The IC50 was found for each compound for each knockout clone using GraphPad Prism.

2.13 Changes made for the competitive growth assay with nutlin-3a and doxorubicin

The clonal knockout cell lines of each INO80 subunit (*UCHL5, NFRKB, INO80*) were grown in the IC30 concentration of nutlin-3a and doxorubicin for 12 days. The IC30 of nutlin-3a is 2μM, and the IC30 of doxorubicin is 5 μM. Relative fitness values for compound treated cells were determined as mentioned above.

Chapter 3 - Results

3.1 Synthetic lethal genome-wide CRISPR screen with BIBR1532 establishes the essentiality of five subunits of the human INO80 complex after telomere erosion

Prior to my joining the Harrington group, a synthetic lethal genome-wide CRISPR screen was performed using the telomerase (*hTERT*) inhibitor BIBR1532 (20 μM) following the methods indicated in Bertomeu *et al* 2017 (Bertomeu *et al*., 2017). In this screen, five of the sixteen subunits of the human INO80 complex were found to impede proliferation in cells treated with BIBR1532 (table 1). These subunits include UCHL5, NFRKB, TFPT, INO80E, and INO80C (table 1). Thus, after the deletion of these subunits in conjunction with the inhibition of telomerase, the cells entered a state of reduced fitness which can be monitored over time by next-generation sequencing of the guide RNAs.

Gene	RANKS Score	FDR
ACTL6A	-0.72	0.902
ACTR5	-1.31	0.567
ACTR8	-0.22	0.979
INO80	-1.24	0.68
INO80B	0.24	0.959
INO80C	-2.33	0.0456
INO80D	-0.34	0.955
INO80E	-2.5	0.0452
MCRS1	-0.09	0.982
NFRKB	-2.88	0.00522
RUVBL1	-0.46	0.955
RUVBL2	N/A	N/A
TFPT	-2.02	0.161
UCHL5	-2.95	0.00456
YY1	-1.35	0.619
YY1AP1	1.05	0.702

Table 1: After treatment with the telomerase inhibitor BIBR1532, cells deleted for the genes encoding certain subunits of the human INO80 complex, individually, demonstrate either a reduced or enhanced fitness.

Five of the sixteen subunits of the human INO80 complex, after knockout, demonstrated a reduced fitness in the presence of BIBR1532, as indicated by a low robust analytics and normalization for knockout screens (RANKS) score and low FDR value. These subunits include UCHL5, NFRKB, INO80E, INO80C and TFPT. Hits were defined as the genes with the lowest 200 scores compared to DMSO controls. RANKS indicate the change in guide RNA frequency over time in the presence of BIBR1532, 20 μM for 20 days, and the FDR values indicate the significance of those RANKS values. The RANKS values and FDR values were determined by following the methods indicated in Bertomeu *et al*, 2017. Data taken from the BIBR1532 screen conducted by Yahya Benslimane, as shown here with permission.

3.2 Some subunits of the human INO80 complex are essential in NALM-6 cells

Each of the sixteen subunits of the human INO80 complex were deleted individually in NALM-6 cells. Each knockout population was then treated with BIBR1532 and DMSO individually (Figure 1a). The relative fitness values of each of the knockout populations were

found and compared to non-targeting control sgRNAs. Relative fitness was determined before and after treatment with BIBR1532 or 0.1 % v/v DMSO. Relative fitness was defined by the ability of the knock out cell lines to grow and divide in order to maintain their population over time. If the subunit was found to have a low relative fitness, the knock out population was not able to proliferate normally compared to non-targeting control knockout cell populations. The fitness values for each knockout population prior to BIBR1532 treatment were found to correlate negatively with the essentiality of each subunit previously determined by Bertomeu *et al*. (Bertomeu *et al*., 2017) (Figure 1b). Thus, the subunits of the human INO80 complex that were found to have a low relative fitness, also showed a strong essentiality in NALM-6 cells. Relative fitness values for each population after BIBR1532 treatment (data from Benslimane, Y el al., unpublished) were shown to correlate negatively with the essentiality of each INO80 subunit in the absence of compound (Bertomeu *et al*., 2017) (Figure 1c).

A

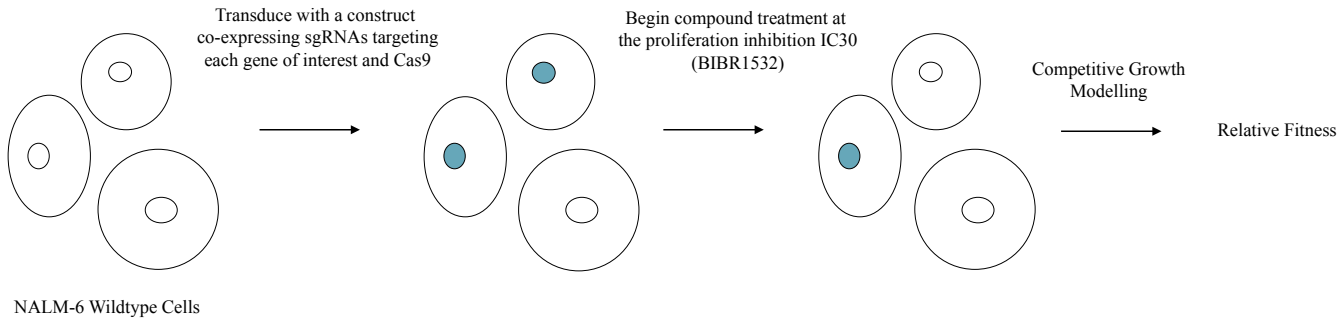
Transduce with a construct
co-expressing sgRNAs targeting
each gene of interest and Cas9
Begin compound treatment at
the proliferation inhibition IC30
(BIBR1532)
Competitive Growth
Modelling
Relative Fitness
NALM-6 Wildtype Cells

B

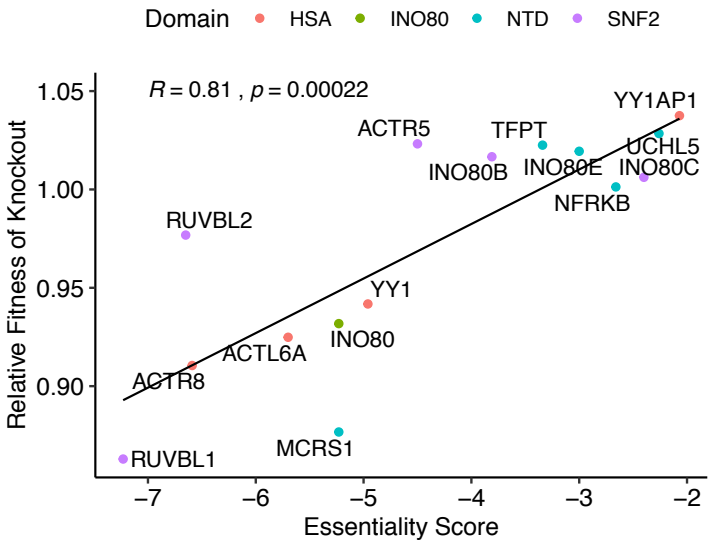
Domain
HSA
INO80
NTD
SNF2
R = 0.81 , p = 0.00022
Relative Fitness of Knockout
Essentiality Score
YY1AP1
ACTR5
TFPT
UCHL5
INO80B
INO80E
INO80C
NFRKB
RUVBL2
YY1
INO80
ACTL6A
ACTR8
MCRS1
RUVBL1

C

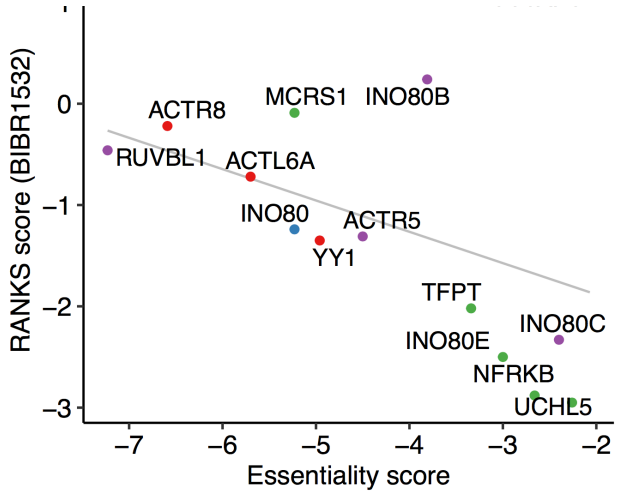
RANKS score (BIBR1532)
Essentiality score
ACTR8
MCRS1
INO80B
RUVBL1
ACTL6A
INO80
ACTR5
YY1
TFPT
INO80C
INO80E
NFRKB
UCHL5

Figure 1 – The essentiality of some subunits of the INO80 complex is altered before and after BIBR1532 treatment in NALM-6 cells.

A) In order to create knockout cell lines of each subunit of the INO80 complex, wildtype NALM-6 cells were transduced with a construct co-expressing sgRNAs targeting each subunit of the INO80 complex individually and Cas9. Next, each population was treated with BIBR1532, the telomerase inhibitor, for 18 days at the IC30 (20 μM). Competitive growth modelling was used to determine the relative fitness of each INO80 subunit knockout population in the presence of BIBR1532. **B)** True knockouts of each of the human INO80 subunits were generated in a population and competitive growth modelling was used to determine the relative fitness, which was analyzed over 12 days, before beginning treatment with BIBR1532. Relative fitness was determined by taking the $\log_2$ ratio of the GFP positive cell ratios (cells that contain the guide RNA to knockout that specific gene) at day 12 versus day 0, and then normalized to wild type cells. The relative fitness values of each knockout without compound treatment demonstrated a positive correlation with the robust analytics and normalization for knockout screens (RANKS) score of essentiality. The RANKS score indicates the fallout rate of guide RNAs targeting that gene in a population of genome wide knockouts, thus the essentiality of that gene. The colours indicate the domain of the INO80 complex for each subunit. Essentiality (RANKS) score taken from Bertomeu *et al*. (Bertomeu *et al*., 2017). R value of 0.81, p = 00022, determined by stat_cor in ggplot (R statistics). The relative fitness of knockout include data from two knockout populations for each gene, represented by two different guide RNAs. **C)** The relative fitness of cells deleted for the genes encoding each INO80 subunit and treated with BIBR1532 negatively correlated with their essentiality in the absence of compound. The RANKS score in BIBR1532 was taken from Benslimane, Y *et al*., unpublished (Data also in Table 1). The essentiality score was taken from Bertomeu *et al*. (Bertomeu *et al*., 2017).

3.3 The deletion of *ACTR5*, *INO80C* or *NFRKB* leads to a reduced relative fitness after telomere erosion caused by BIBR1532 treatment

Each individual NALM-6 population of a knockout of a single subunit of the human INO80 complex was treated with 20 μM BIBR1532. I chose this concentration because, prior to my joining the lab, 20 μM was determined to be the IC30 concentration of BIBR1532, or the concentration at which there is 30% inhibition of proliferation (Y. Benslimane, unpublished). All 16 populations were treated with BIBR1532 for 18 days in addition to a non-targeting control knockout population. A significant reduction in relative fitness compared to a non-targeting control knockout population was found in knockout populations of *ACTR5*, *INO80C* and *NFRKB* (Figure 2).

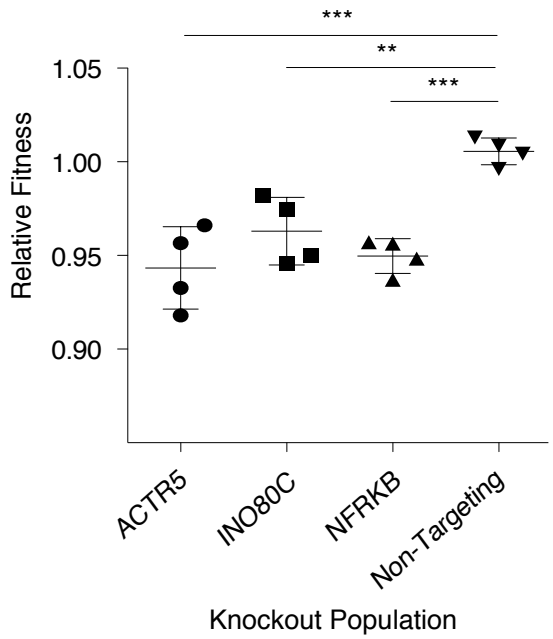

Figure 2 - Significant decreases in relative fitness occur after deletions of *ACTR5*, *INO80C* and *NFRKB* individually with BIBR1532 treatment over 18 days. Each cellular population included one of the above knockouts and were each treated with 20 μM BIBR1532 for 18 days in order to determine changes in relative fitness compared to DMSO treatment. The relative fitness of each knockout cell line in BIBR1532 was determined by finding the ratio of $\log_2$ value of GFP positive cell ratios over time and normalizing to the proliferation of those cell knockout cell lines in DMSO. Those values were then added to the wildtype proliferation rate of NALM-6 cells (1.25 cellular doublings per day). Statistical analysis was carried out using a one-way analysis of variance (ANOVA) and a Dunnett's multiple comparison test. This data includes two biological replicates (two knockout populations for each gene represented by different guide RNAs) and two technical replicates of the experiment. Data are represented as mean +/- SD. ** represents $p<0.01$, *** represents $p<0.001$.

3.4 Clonal cell lines deleted for the gene encoding the enzymatic subunit of telomerase (*hTERT*) cannot divide indefinitely

NALM-6 cells were deleted for the enzymatic subunit of human telomerase (*hTERT*), knockout clones selected for and grown and further monitored for cellular divisions. Cell densities were determined every three days and plotted over time for each confirmed knockout clonal cell lines. The proliferation of each *TERT* knockout clonal cell line plateaued after around 25-30 days in culture (Figure 3). Some of the cell lines arrested proliferation after 40 days in culture, thus, these clones allowed for an optimal amount of time in order for further experimentation to occur. After the deletion of *hTERT* and clonal selection, clone 2 was chosen for further experimentation due to its long lifespan (Figure 3).

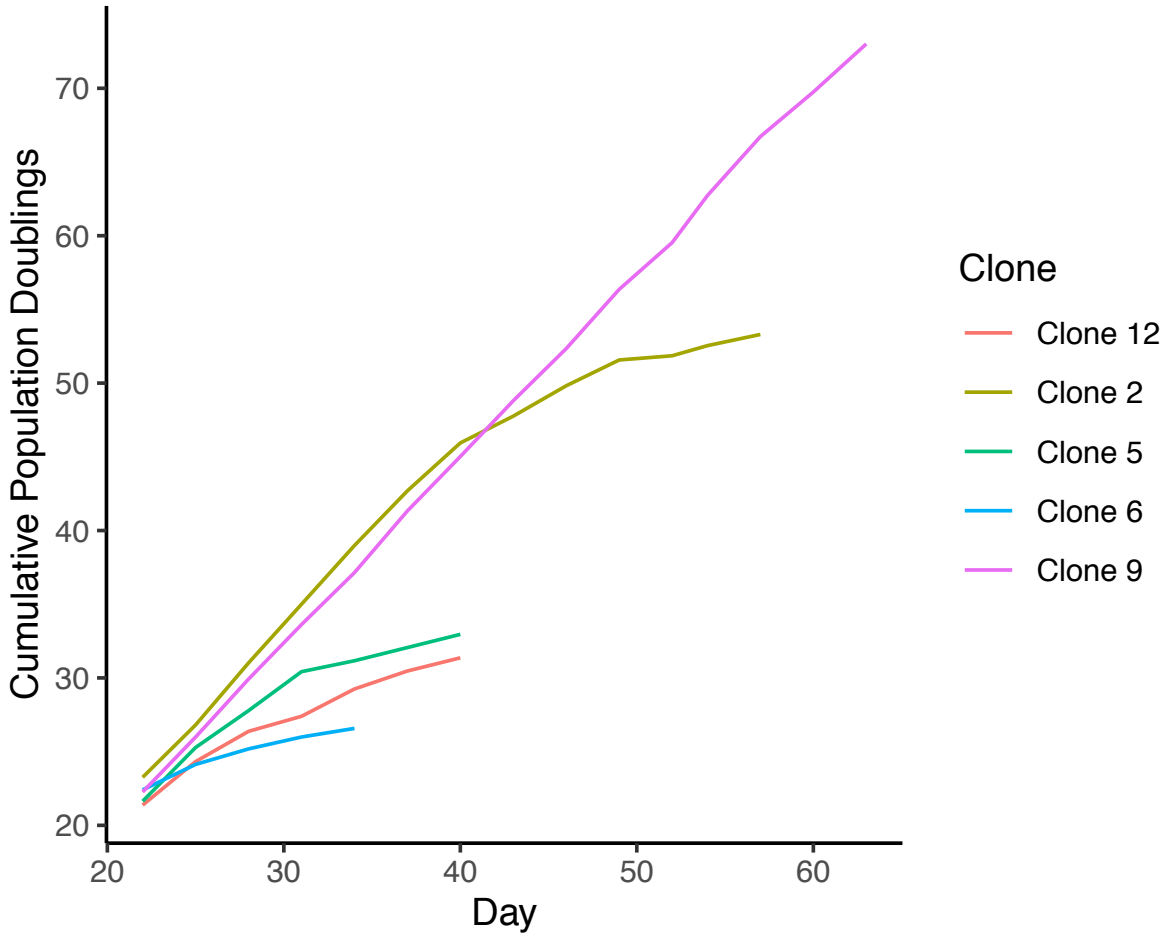

Figure 3 - Decreases in proliferation occur after the deletion of *hTERT* in NALM-6 cells. NALM-6 cells clonally deleted for *hTERT* were selected by dilution and grown in culture until cellular proliferation was arrested for each clonal cell line. Population doubling level was determined by the $\log_2$ ratio of the cell density day 3 vs the cell density at day 0 etc., and repeats for each cell passage. Cumulative population doublings were tracked over time for each *hTERT* knockout clonal cell line.

3.5 The relative fitness of cells deleted for telomerase is lower after treatment with UCHL5 inhibitors

Overall, relative fitness was lowered in cells deleted for some subunits of the human INO80 complex in conjunction with BIBR1532 treatment. Thus, I set out to determine whether the reciprocal scenario, *hTERT* deletion with INO80 subunit chemical inhibition, replicated the observed synthetic lethality between the abrogation of both telomerase and INO80. In order to determine whether the synthetic lethality observed using telomerase inhibition with BIBR1532 was specific to telomerase, cells deleted for *hTERT* were treated with the UCHL5 inhibitor NSC-687852 or WP-1130 at the IC30 (Figure 4a,b). After the deletion of *hTERT* and chemical inhibition of UCHL5, a subunit of the INO80 complex, relative fitness was diminished after 6 days (Figure 4c). Chemical inhibition of UCHL5 was chosen to represent chemical inhibition of the human INO80 complex as these inhibitors are widely available and have limited off-target effects. Additionally, the deletion of *UCHL5* was shown to be consistently synthetic lethal with the inhibition of telomerase throughout many experiments.

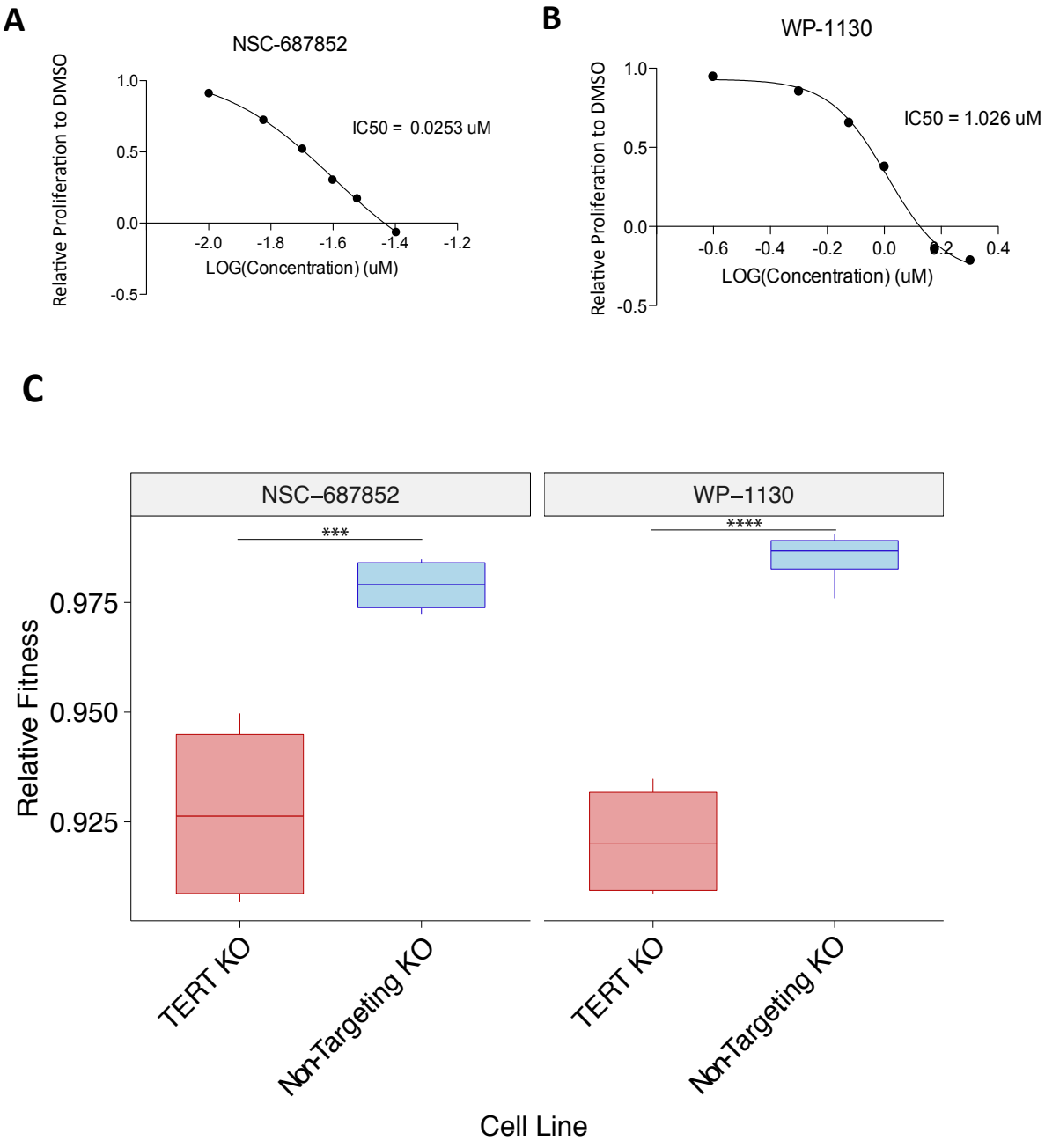
A
NSC-687852
Relative Proliferation to DMSO
IC50 = 0.0253 uM
LOG(Concentration) (uM)
B
WP-1130
Relative Proliferation to DMSO
IC50 = 1.026 uM
LOG(Concentration) (uM)
C
NSC–687852
WP–1130
***
****
Relative Fitness
TERT KO
Non-Targeting KO
TERT KO
Non-Targeting KO
Cell Line

Figure 4 - Significant decreases in relative fitness occur after the clonal deletion of *hTERT* in addition to NSC-687852 or WP-1130 treatment (UCHL5 chemical inhibitors) after 6 days. A – The proliferation of NALM-6 cells was reduced after treatment with NSC-687852 in a dose-dependent manner. Wild-type NALM-6 cells were treated with NSC-687852 at varying concentrations (0.01 μM, 0.015 μM, 0.02 μM, 0.025 μM, 0.03 μM, and 0.04 μM) as well as 0.01% DMSO. Population doublings were determined by finding the log2 ratio of cell density at day 3 compared to day 0. Relative proliferation was then found by normalizing cell doublings to those in DMSO. The IC30 of NSC-687852 was determined to be 0.02 μM, or the concentration at which approximately 30% inhibition of proliferation occurs to wild-type NALM-6 cells. The IC50 indicated was calculated by Graphpad Prism. **B** - The proliferation of NALM-6 cells was reduced after treatment with WP-1130 in a dose-dependent manner. Wild-type NALM-6 cells were treated with WP-1130 at varying concentrations (0.25 μM, 0.5 μM, 0.75 μM, 1 μM, 1.5 μM, and 2 μM) as well as 0.01% v/v DMSO. Population doublings were determined by finding the log2 ratio of cell density at day 3 compared to day 0. Relative proliferation was then found by normalizing cell doublings to those in DMSO. The IC30 of WP-1130 was determined to be 1 μM. The IC50 indicated was calculated by Graphpad Prism. **C** – After 6 days of either NSC-687852 or WP-1130 treatment at the IC30, the relative fitness of *TERT* knockout clonal cells was lower than that of wild-type cells (non-targeting controls). Relative fitness was determined by finding the ratio of $\log_2$ value of GFP positive cell ratios over time and normalizing to the proliferation of those cell knockout cell lines in DMSO. Statistical analysis was carried out using a one-way ANOVA and multiple comparison test. *** represents $p<0.001$, **** represents $p<0.0001$. The data include two technical replicates of the experiment, and within each, two biological replicates (two knockout clonal cell lines for each genotype, represented by two different guide RNAs.

3.6 The relative fitness of cells deleted for both telomerase and some subunits of the human INO80 complex is lower than wildtype cells

After the deletion of *hTERT* and clonal selection, clone 2 was chosen for further experimentation due to its long lifespan (Figure 3). This *hTERT* knockout clonal cell line was then deleted for each INO80 subunit individually at the population level, to create 16 different cell lines. These double knockout cell lines were then monitored over 24 days. The relative fitness values of the following double knockout combinations were lowered: *ACTR8-hTERT*, *INO80-hTERT*, *INO80B-hTERT*, *NFRKB-hTERT*, and *UCHL5-hTERT* (Figure 5a). Over time, this synthetic lethality can be observed to occur between day 21-24 (Figure 5b). In summary, synthetic lethality can be observed between the loss of telomerase and certain subunits of the INO80 complex with both chemical inhibition or genetic deletion.

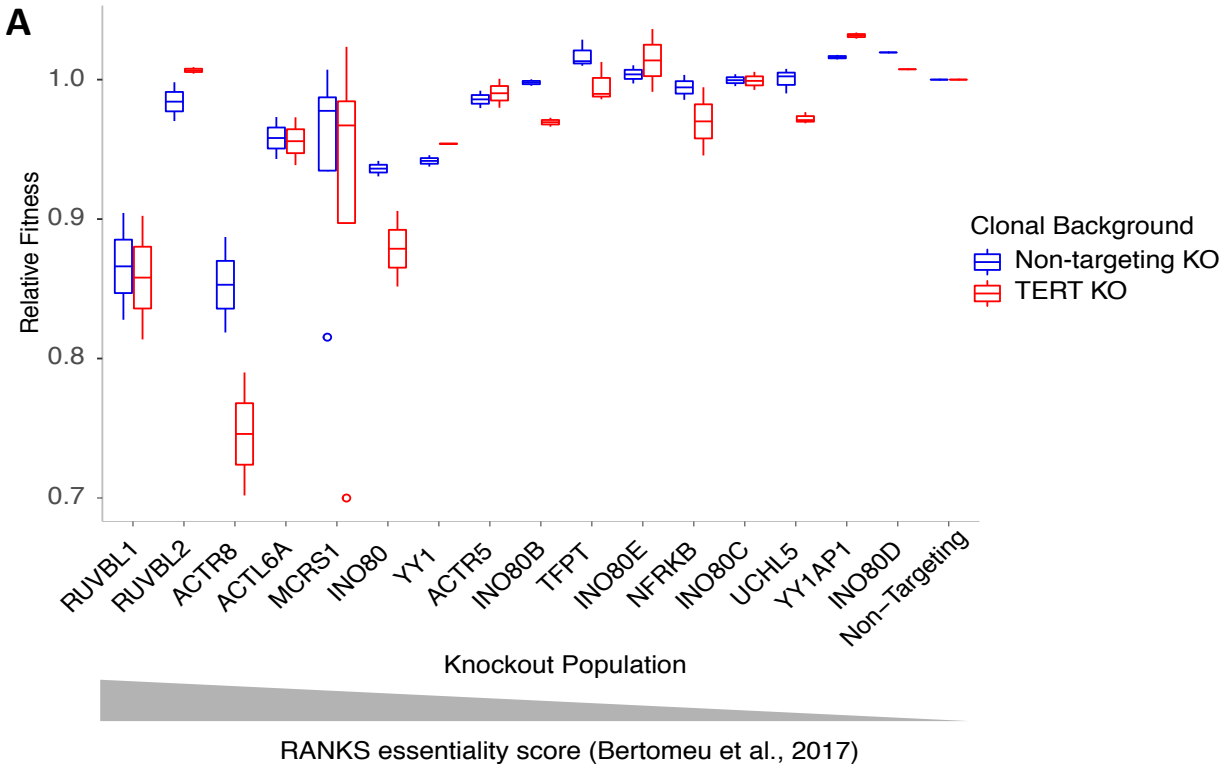
A
Relative Fitness
1.0
0.9
0.8
0.7
RUVBL1
RUVBL2
ACTR8
ACTL6A
MCRS1
INO80
YY1
ACTR5
INO80B
TFPT
INO80E
NFRKB
INO80C
UCHL5
YY1AP1
INO80D
Non−Targeting
Knockout Population
RANKS essentiality score (Bertomeu et al., 2017)
Clonal Background
Non-targeting KO
TERT KO

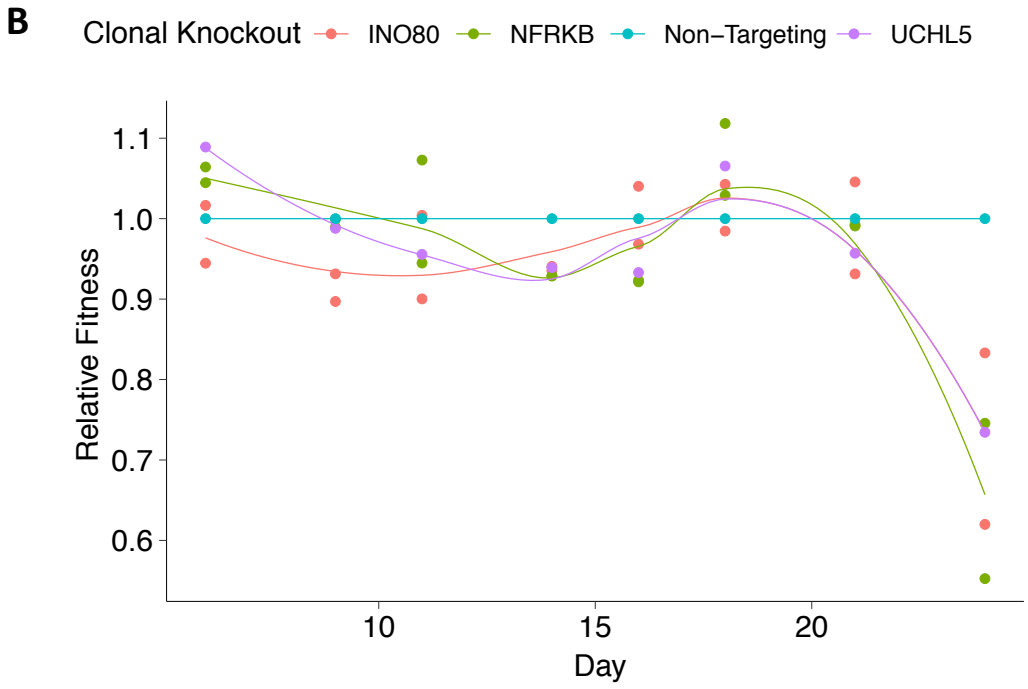
B
Clonal Knockout
INO80
NFRKB
Non−Targeting
UCHL5
Relative Fitness
1.1
1.0
0.9
0.8
0.7
0.6
10
15
20
Day

Figure 5 – Decreases in relative fitness occur after deletions of *ACTR8, INO80, INO80B, NFRKB* and *UCHL5* individually with the deletion of *TERT* over 24 days. A – Between day 3 and day 24, the relative fitness of cells deleted for *ACTR8, INO80, INO80B, NFRKB* or *UCHL5* in the presence of a telomerase clonal knockout was lowered. Relative fitness was determined by finding the $\log_2$ ratio of the proportion of GFP positive cells at day 24 vs day 3. This slope was then added to the proliferation value of the background clonal cell line (either telomerase knockout clonal cell line or non-targeting control cell line). This growth value was then normalized to the growth value of the background clonal cell line (either telomerase knockout clonal cell line or non-targeting control cell line). The subunits were organized based on essentiality as determined by Bertomeu *et al* (Bertomeu *et al*., 2017). This data includes approximately two biological replicates, represented by approximately two guide RNAs for each knockout population. **B** – The reduction in relative fitness observed in the above double knockouts was observed after day 21. The instantaneous relative fitness values were determined as above, however, the slope was determined for every three days. This data includes approximately two biological replicates, represented by approximately two guide RNAs for each knockout population.

3.7 p53 target expression levels are increased after the deletion of telomerase (*hTERT*) and treatment with the p53 stabilizer, nutlin-3a

In order to determine the mechanism behind the observed changes in relative fitness, it was hypothesized that the p53 pathway is implicated in cellular growth arrest, and this pathway is targeted and amplified in response to chemical or genetic ablation of telomerase or INO80 complex function. The stimulation of the p53 pathway in cells modified for telomerase or INO80 function may lead to cellular growth arrest. It has also been noted that the INO80 complex may act as a repressor of *CDKN1A* transcription. We hypothesize that the alterations in p53 target expression levels after telomerase loss are additive to the alterations in p53 target expression levels after the INO80 complex loss, leading to enhanced rates of growth arrest.

In order to determine whether there are changes in p53 target expression levels after either the stimulation of p53, the loss of telomerase or the inhibition of UCHL5, telomerase knockout populations were first sorted for the cells expressing the telomerase knockout construct, and then treated with the IC30 of either the p53 stimulator nutlin-3a, or UCHL5 inhibitors NSC-687852 or WP-1130. Nutlin-3a acts as an inhibitor of *MDM2*, thus stabilizing p53 (Vassilev *et al*., 2004). The IC50 determination of nutlin-3a is represented in Figure 8. After the deletion of telomerase, *CDKN1A*, *BAX* and *MDM2* expression was increased (Figure 6). After 6 days of nutlin-3a treatment, *CDKN1A* and *MDM2* expression increased in cells deleted for telomerase (Figure 6). After 6 days of NSC-687852 treatment, no expression changes are observed compared to DMSO treated cells (Figure 6). After 6 days of WP-1130 treatment, no expression changes are observed compared to DMSO treated cells (Figure 6).

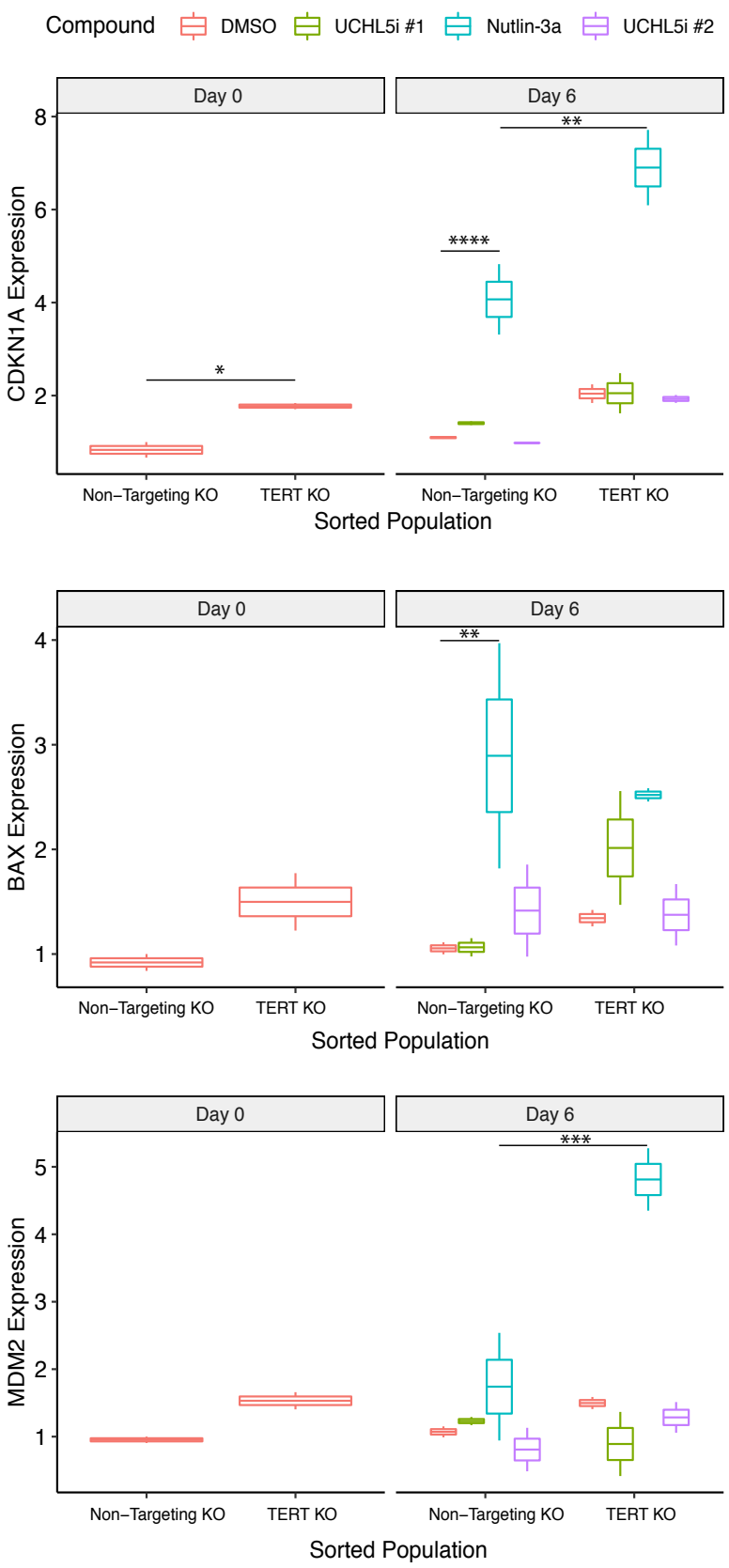
Compound
DMSO
UCHL5i #1
Nutlin-3a
UCHL5i #2
Day 0
Day 6
CDKN1A Expression
BAX Expression
MDM2 Expression
Non−Targeting KO
TERT KO
Sorted Population
*
**
****
***

Figure 6 - p53 target expression is altered after the deletion of *TERT* in combination with p53 stabilization. *TERT* knockout populations (kindly generated and provided by Y. Benslimane) were sorted for GFP positive cells and then treated with DMSO (0.1% v/v), NSC-687852, WP-1130 or nutlin-3a for 6 days (all compounds at the IC30). IC50 determination of nutlin-3a is represented in Figure 8. *CDKN1A* expression is increased after the deletion of *TERT* and further increased after the deletion of *TERT* in addition to nutlin-3a treatment for 6 days. 6 days of nutlin-3a treatment increased *CDKN1A* and *BAX* expression in non-targeting control cell lines. *MDM2* expression is increased after the deletion of *TERT* in addition to nutlin-3a treatment for 6 days. Expression levels correspond to mRNA levels determined by qPCR normalized to the housekeeping genes *HPRT* and *GAPDH*. The IC30 of NSC-687852 was 0.02 μM, the IC30 of WP-1130 was 1 μM and the IC30 of nutlin-3a was 2 μM. These data represent two biological replicates for each clonal knockout background cell line. Statistical analysis was carried out using one-way ANOVA, and Sidak's multiple comparison analysis was performed separately for day 0 and day 6 data. * represents $p<0.05$, ** represents $p< 0.01$, *** represents $p<0.001$, **** represents $p<0.0001$.

3.8 p53 target expression is increased after the deletion of some subunits of the human INO80 complex and treatment with the p53 stabilizer, nutlin-3a

Due to the changes observed in p53 target expression after nutlin-3a treatment for 6 days, nutlin-3a treatment was carried out for a shorter time course to determine whether p53 target expression changes also occur. NALM-6 clones deleted for certain subunits of the human INO80 complex, INO80 (heterozygous knockout), *NFRKB* or *UCHL5* (homozygous knockouts), were treated with the p53 stabilizer, nutlin-3a for 4 hours at the IC30 concentration (2 μM), and the expression levels of p53 targets were examined. After nutlin-3a treatment for 4 hours, a significant increase in *CDKN1A* and *MDM2* expression was observed in cells deleted for *NFRKB* (Figure 7). In addition, after nutlin-3a treatment for 4 hours, *MDM2* expression significantly increased in cells deleted for *UCHL5* (Figure 7c).

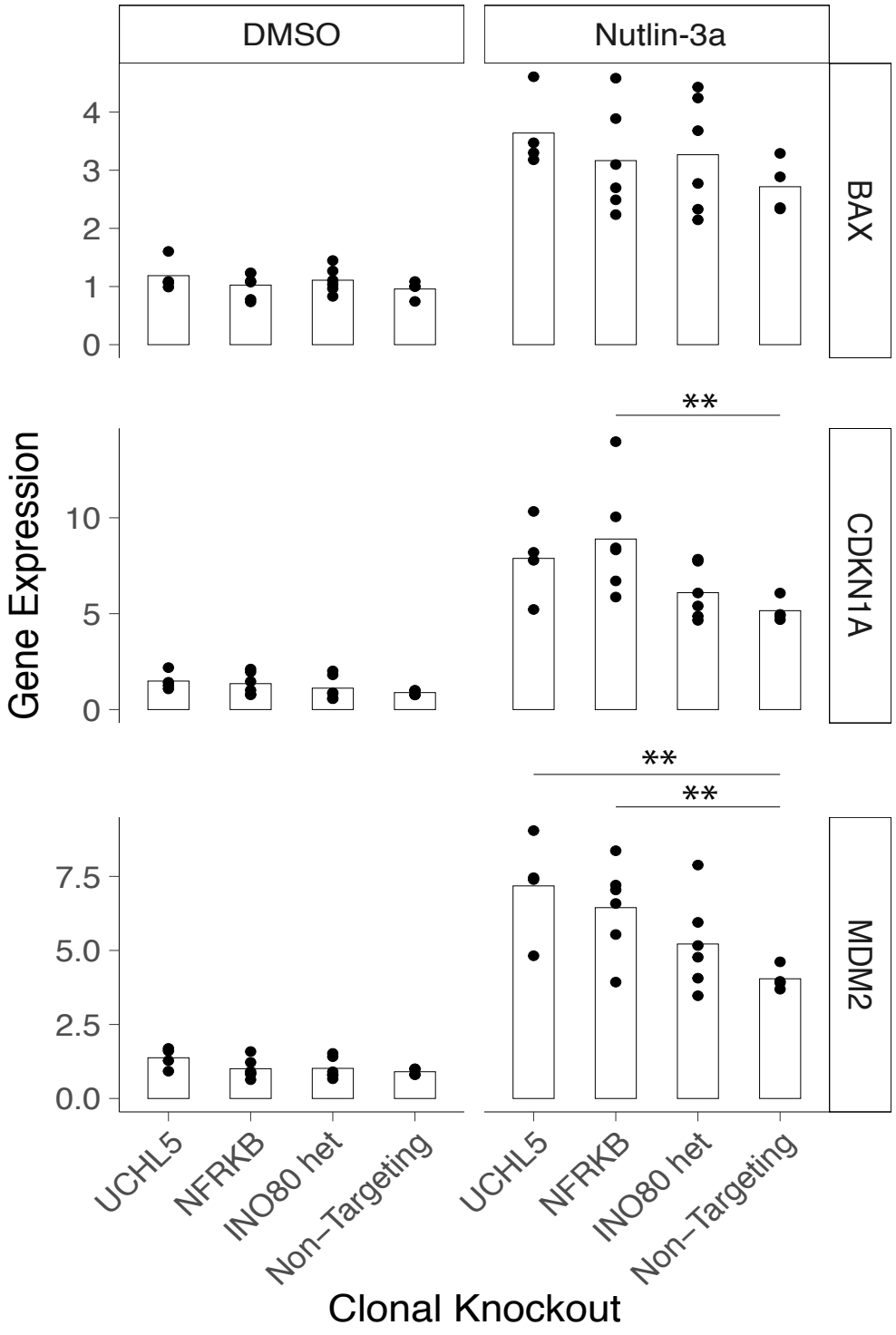
DMSO
Nutlin-3a
BAX
CDKN1A
MDM2
Gene Expression
**
**
**
0
1
2
3
4
0
5
10
0.0
2.5
5.0
7.5
UCHL5
NFRKB
INO80 het
Non−Targeting
Clonal Knockout

Figure 7 - p53 target expression is altered after the deletion of some subunits of the INO80 complex and nutlin-3a treatment. *BAX* expression increased after 4 hours of nutlin-3a treatment compared to DMSO treatment. INO80 subunit deletion did not alter *BAX* expression. *CDKN1A* expression increased after 4 hours of nutlin-3a treatment compared to DMSO treatment. *NFRKB* deletion increased the expression of *CDKN1A* only after 4 hours of nutlin-3a treatment compared to non-targeting controls. *MDM2* expression increased after 4 hours of nutlin-3a treatment compared to DMSO treatment. *NFRKB* and *UCHL5* deletion individually increased *MDM2* expression only after 4 hours of nutlin-3a treatment compared to non-targeting controls. Nutlin-3a treatment was performed at the IC30 (2 μM) as determined by Benslimane, Y unpublished. Gene expression of *BAX*, *CDKN1A* and *MDM2* were determined by qPCR and normalized to the expression values of the housekeeping genes *HPRT* and *GAPDH*. These data include two biological replicates (two knockout clonal cell lines for each genotype) and two technical replicates. The qPCR wells were in triplicate. Statistical analysis was performed using Graphpad software, and a one-way ANOVA and multiple comparison test was used to determine statistical significant differences. ** represents $p<0.01$. Statistical analysis was performed for each gene separately.

3.9 The IC50 of the p53 stabilizers, nutlin-3a and doxorubicin is lowered after the deletion of some subunits of the human INO80 complex

The NALM-6 clones deleted for certain subunits of the human INO80 complex (*INO80*, *NFRKB* or *UCHL5*) were then treated with either nutlin-3a or doxorubicin at many different concentrations each. Proliferation of each treatment and concentration and each cell line was determined after 4 days, and the IC50 for each compound and each cell line was determined. Doxorubicin is a commonly used anti-cancer agent that inhibits topoisomerase2b which leads to reactive oxygen species (ROS) accumulation and a p53 apoptotic response (Tewey *et al*., 1984, Zhang *et al*., 2012). NALM-6 clones deleted for *NFRKB* were found to have a lower IC50 of doxorubicin when compared to non-targeting control knockout clonal cell lines (Figure 8a). NALM-6 clones deleted for *UCHL5* were found to have a lower IC50 of nutlin-3a when compared to non-targeting control knockout clonal cell lines (Figure 8b). Thus, the proliferation of *NFRKB* knockout clones was lowered in the presence of doxorubicin, and the proliferation of *UCHL5* knockout clones was lowered in the presence of nutlin-3a.

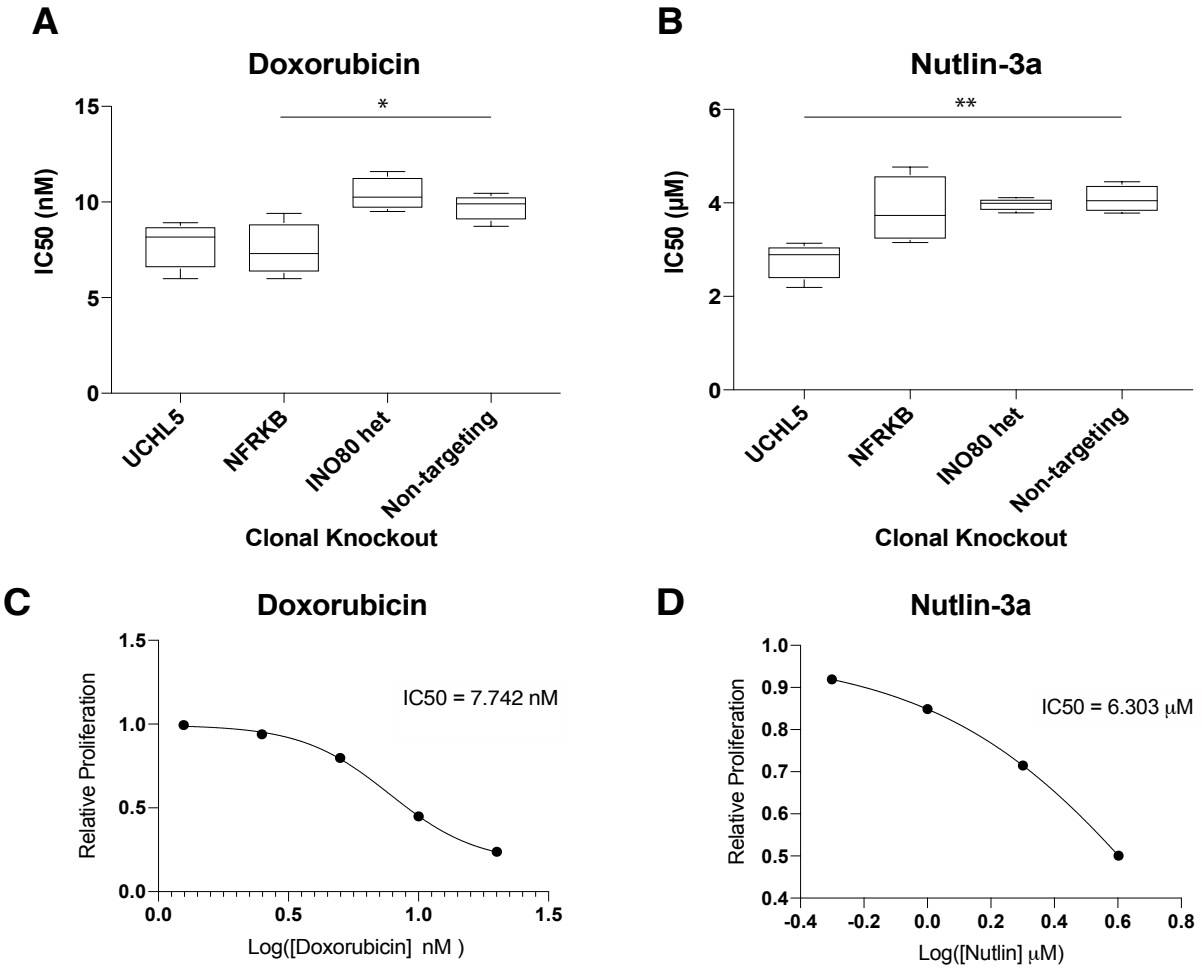

Figure 8 - The deletion *NFRKB* or *UCHL5* lead to a lower IC50 of p53 altering compounds. **A** - In the presence of varying concentrations of doxorubicin (1.25 nM, 2.5 nM, 5 nM, 10 nM, 20 nM) for 4 days, *NFRKB* knockout clones had a significantly lower IC50 than non-targeting controls ($p = 0.037$). **B** - In the presence of varying concentrations of nutlin-3a (0.5 μM, 1 μM, 2 μM, 4 μM) for 4 days, *UCHL5* knockout clones had a significantly lower IC50 than non-targeting controls ($p = 0.0044$). Relative proliferation was determined by finding the population doubling level of each cell line in each treatment group after 4 days (Population Doublings = $\log_2$(cell density day 4/cell density day 0)) and then dividing the population doubling level to that found in the cell line treated with 0.1% DMSO. Statistical analysis included IC50 determination via non-linear fit analysis on Graphpad, a one-way ANOVA of IC50 values and a Dunnett's multiple comparison test. * represents $p<0.05$, ** represents $p<0.01$. **C** The IC50 of doxorubicin

was found to be 7.742 nM in wild-type NALM-6 cells. Two non-targeting knockout clonal cell lines (D11-1, D11-7) were treated with the varying concentrations of doxorubicin (1.25 nM, 2.5 nM, 5 nM, 10 nM, 20 nM) and relative proliferation was measured after 4 days as indicated above. **D** The IC50 of nutlin-3a was found to be 6.303 μM in wild-type NALM-6 cells. Two non-targeting knockout clonal cell lines (D11-1, D11-7) were treated with the varying concentrations of nutlin-3a (0.5 μM, 1 μM, 2 μM, 4 μM) and relative proliferation was measured after 4 days as indicated above. These data (**A-D**) include two biological replicates (two knockout clonal cell lines for each genotype) and two technical replicates. INO80 clonal knockout cell lines were only heterozygote knockouts, rather than homozygote knockouts.

3.10 Cellular proliferation is decreased after the deletion of *UCHL5* or *NFRKB* and treatment with the p53 stabilizers, nutlin-3a or doxorubicin

Overall, p53 target expression has been shown to be altered after Nutlin-3 treatment or doxorubicin in addition to the deletion of certain subunits of the human INO80 complex. Thus, synthetic lethality between p53 chemical stimulation and INO80 inhibition may be observed. Populations of cells deleted for either *INO80*, *UCHL5* or *NFRKB* were then treated with either nutlin-3a or doxorubicin at the IC30 for 12 days. The relative fitness of cells deleted for either *UCHL5* or *NFRKB* was reduced in the presence of Nulin-3a or doxorubicin for 12 days (Figure 9).

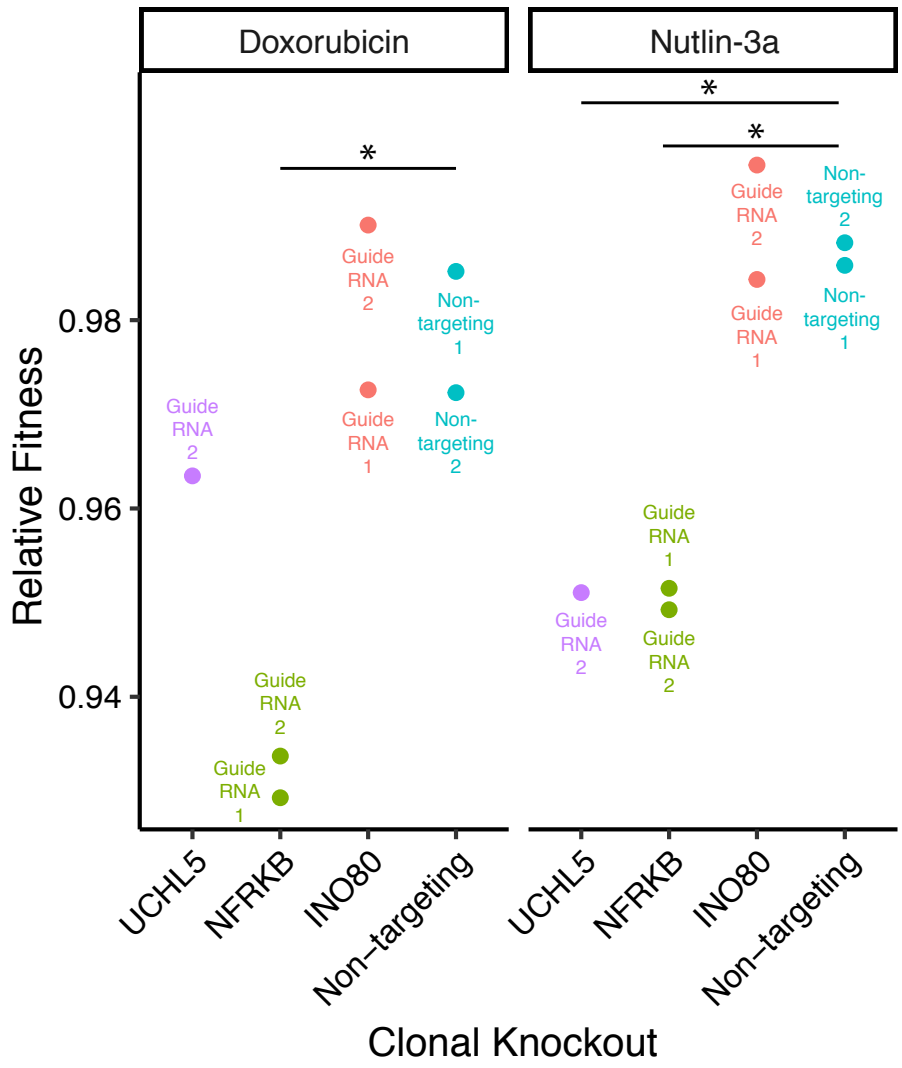

Figure 9 – The relative fitness of cells deleted for *UCHL5* or *NFRKB* is lowered in the presence of doxorubicin or nutlin-3a. The clonal knockout cell lines of each INO80 subunit (*UCHL5, NFRKB, INO80*) were grown in the IC30 concentration of nutlin-3a and doxorubicin for 12 days. The relative fitness of the cells deleted for *NFRKB* was significantly lower than non-targeting control cell lines after doxorubicin treatment, as determined by one-way ANOVA and a Dunnett's multiple comparison test ($p = 0.0298$). The relative fitness values of the cells deleted for *NFRKB* or *UCHL5* were significantly lower than non-targeting control cell lines after nutlin-3a treatment, as determined by one-way ANOVA and a Dunnett's multiple comparison test ($p = 0.0125, 0.0233$ respectively). Relative fitness was determined by finding the ratio of $\log_2$ value

of GFP positive cell ratios over time and normalizing to the proliferation of those cell knockout cell lines in DMSO (0.01% v/v). The IC30 of nutlin-3a is 2μM, and the IC30 of doxorubicin is 5 μM. Each genotype contained two knockout clonal cell lines each, guide RNA 1 and 2 (two biological replicates). Statistical analysis was performed after the removal of guide RNA 1 for *UCHL5* (I25) from the data. * represents $p<0.05$.

Chapter 4 - Discussion

4.1 Synthetic lethality is observed after inhibition of telomerase and certain subunits of the human INO80 complex

This study investigated the potential synthetic lethal relationship between the loss of telomerase and certain subunits of the human INO80 complex, as identified in a genome-wide CRISPR screen investigating protein essentiality changes after telomere erosion. We first set out to determine whether there is a reduction in relative fitness after the chemical or genetic interruption of the human INO80 complex function in addition to the loss of telomerase (*hTERT*).

Here it is shown that knockout populations of each subunit of the human INO80 complex were created, and knockout populations of certain subunits (e.g. *RUVBL1*) demonstrated a reduced relative fitness. These subunits were also found to be essential based on previous results by Bertomeu *et al*. (Bertomeu *et al*., 2017). Due to the correlation between the relative fitness of the knockout populations and the essentiality previously defined of each subunit, it can be concluded that the loss of certain subunits of the human INO80 complex is detrimental to survival of the cell to varying extents.

It has been noted that the human INO80 complex serves many purposes within the cell. As the complex functions primarily to maintain the chromatin landscape by altering the position of histones, specifically unacetylated H2A.Z, this complex is essential for genomic integrity in yeast (Papamichos-Chronakis *et al*. 2011). The INO80 complex was also shown to be important for the removal of H2A.Z during transcriptional activation (Papamichos-Chronakis *et al*. 2011). Specific subunits may be essential for these functions, and thus, the loss of these specific subunits results in cellular growth arrest. Essentiality values for each of the subunits are described in Table 2. Here it was determined that the more essential subunits include RUVBL1, RUVBL2, ACTR8, MCRS1, ACTL6A, INO80 and YY1. In addition, when choosing clonal knockouts of the core enzymatic subunit *INO80*, only heterozygote knockout clones arose. This result suggests that homozygote knockout clones are inviable. Previously, it has been shown that subunits, such as YY1, are essential for development, and the loss is therefore lethal (Affar *et al*., 2006). Essentiality of each subunit in different contexts was examined in Table 2. As many of

the subunits of the human INO80 complex are essential, knockout cell lines are inviable, and thus relative fitness and synthetic lethality is not possible to analyze. This result may be why not all of the subunits of the INO80 complex after deletion were found to be synthetic lethal with the loss of telomerase. In addition, as the essentiality of the subunits vary, a negative correlation was found between the essentiality of each subunit as determined by Bertomeu *et al*, and the essentiality of each subunit in the presence of BIBR1532 (Bertomeu *et al*., 2017). Thus, most of the original hits identified as synthetic lethal with the loss of telomerase (*hTERT*) in the genome-wide CRISPR screen were not essential. This result may be another reason why we were not able to identify all subunits of the human INO80 complex as synthetic lethal with the inhibition of telomerase. It may be difficult to determine additional fitness defects if the subunit is already essential within the cell, given the experimental context.

Finally, relative fitness values were determined in a variety of ways throughout the above experiments. Further experimentation and analysis must be done to determine the most accurate method for determining changes in fitness levels of both single and double knockout populations.

Subunit/Gene	RANKS Score (Bertomeu *et al*., 2017)	RANKS Score after BIBR1532 treatment (Benslimane, Y., unpublished)	Gene Effect (CERES) by CRISPR
ACTL6A	-5.7	-0.72	~ -1.5
INO80B	-3.81	0.24	~ -0.5
YY1	-4.96	-1.35	~ -0.75
ACTR5	-4.5	-1.31	~ -0.5
INO80C	-2.4	-2.33	~ -0.2
INO80	-5.23	-1.24	~ -0.5
ACTR8	-6.59	-0.22	~ -1.0
YY1AP1	-2.07	1.05	~ -0.1
UCHL5	-2.26	-2.95	~ -0.5
NFRKB	-2.66	-2.88	~ -0.7
RUVBL2	-6.65	N/A	~ -1.6
INO80E	-3	-2.5	~ -0.25
MCRS1	-5.23	-0.09	~ -0.5
RUVBL1	-7.23	-0.46	~ -1.8
TFPT	-3.34	-2.02	~ -0.3
INO80D	-2.06	-0.34	~ 0.1

Table 2: The essentiality of each INO80 subunit varies.

Positive correlations can be observed for the RANKS score (Bertomeu *et al*., 2017) and the Gene Effect Score (CERES) by CRISPR (Avana) public 20Q1 (data available at https://depmap.org/portal/). CERES is described as the gene dependency score found by CRISPR-Cas9 essentiality screens, and is reported the approximate peak (mode) of the normal distribution of available data. RANKS Score after BIBR1532 treatment was taken from Benslimane, Y, unpublished.

After the inhibition of telomerase function by using the chemical inhibitor BIBR1532 in conjunction with the deletion of each subunit of the INO80 complex individually, a reduced relative fitness was observed in populations that were deleted for *ACTR5*, *INO80C* or *NFRKB* (Figure 3). Additionally, after the chemical inhibition of UCHL5 by NSC-687852 or WP-1130 and the deletion of the enzymatic subunit of telomerase, a reduced relative fitness was observed (Figure 5). Finally, after the clonal selection of NALM-6 cells deleted for telomerase and further deleted for each subunit of the human INO80 complex individually, a reduction of relative fitness was observed in those populations deleted for *ACTR8, INO80, INO80B, NFRKB* and *UCHL5* (Figure 6a).

A caveat of the CRISPR system involves the efficiency of each guide RNA used. Guide RNA indel efficiencies are listed in Supplementary Figure S3. Not all guides had a high indel efficiency, as defined by the ICE score, or the percentage of sequencing reads containing an insertion or deletion in the population, divided by the percentage of the population that is GFP positive. Essential subunits do not contain a high indel efficiency as the cells that contain the guide RNA are quickly selected out of the population. Also, non-essential subunits may have cells that express GFP but do not contain an indel, or may contain a non-frameshift mutation, and are thus, wildtype for the protein of interest. This fact may cause inaccuracy among the data, as knockouts are followed by the presence of GFP in the cell in the experiments contained within this thesis.

The observed synthetic lethal phenotype might be explained by a variety of interdependencies between telomere integrity and chromatin regulation. If the loss of either pathway provides an extra sensitivity to the loss of the other pathway, then one pathway may be a coping mechanism for the loss of the second pathway. Many hypotheses for the potential coping mechanisms are as follows. The INO80 complex has been shown to play a repressive role in the transcription of stress response genes in yeast (Klopf *et al*., 2009). Thus, after the loss of telomerase, and the stress response induced by short telomeres, the role of INO80 in transcriptional repression may reflect a greater importance for cell survival. If stress response genes are activated at a higher rate after both the loss of telomerase in addition to the loss of the INO80 complex function, it is possible that the cell undergoes growth arrest more quickly. Another possibility is that after the loss of telomerase, the INO80 complex is essential for the double strand break repair that is required if the ends of chromosomes are recognized as double

strand breaks. After the double strand break response is initiated, homologous recombination ensues (Lademann *et al*., 2017). It has been shown that the INO80 complex is important for the switch between RPA and RAD51 bound to the DNA during repair (Lademann *et al*., 2017). Thus, if telomerase is lost, and the telomeres are recognized as double strand breaks, the function of the INO80 complex may be important in the DNA damage response. If the INO80 complex is also lost, the cells may not be able to undergo efficient and necessary DNA damage repair, and might undergo growth arrest. Moreover, the human INO80 complex has been proposed to act as a repressor of *CDKN1A* transcription in a p53 dependent manner. The loss of telomerase has also been shown to induce a p53 response (Chin *et al*., 1999, Herbig *et al*., 2004). Thus, the expression of p21 has been shown to increase with both the loss of telomerase or the loss of the human INO80 complex. Overall, the loss of both pathways may be additive in the expression increase of p21, leading to a quicker growth arrest. This final hypothesis was investigated within this report.

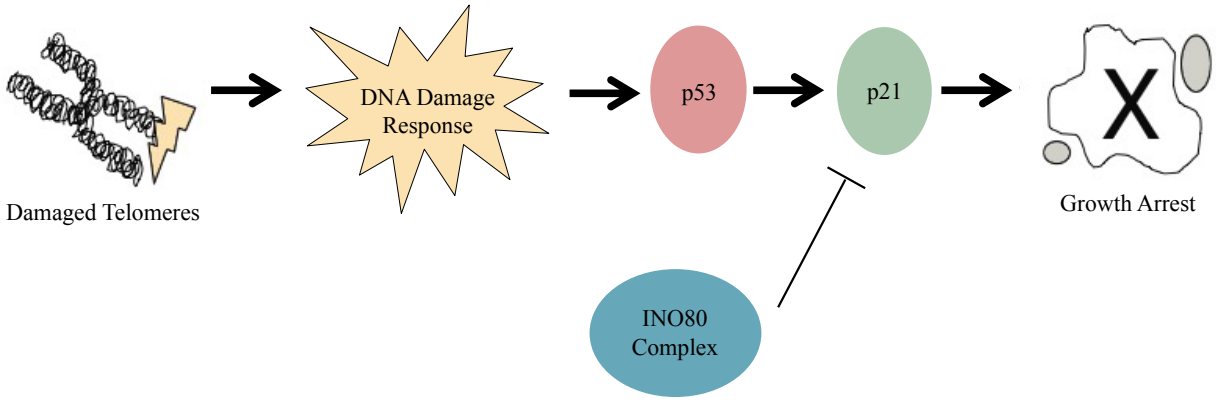

Schematic 3: Critically short telomeres have been shown to induce a DNA damage response leading to p53/p21 mediated growth arrest. Previous reports have reported the inhibition of transcription of *CDKN1A* by the human INO80 complex (Cao *et al*., 2015). If the cell loses the functions of both telomerase and the INO80 complex, the expression changes of p21 may be additive leading to a quicker growth arrest.

4.2 A reduction in relative fitness was observed with the deletion of both telomerase (*hTERT*) and some subunits of the human INO80 complex after 21 days

I then wished to determine whether the synthetic lethal phenotype observed was dependent on time. After NALM-6 cells were clonally selected for knockouts of telomerase, and then deleted for each subunit of the human INO80 complex in individual populations, the reduction in relative fitness that occurred commenced after day 21 (Figure 6b). The observed synthetic lethality between the loss of telomerase and these specific subunits of the human INO80 complex (NFRKB, UCHL5 and INO80) occurred between day 21-24 after the onset of each knockout. This time period also coincides with the loss of cellular proliferation of cells clonally deleted for the enzymatic subunit of telomerase (Figure 4). The cells deleted for *hTERT* begin to plateau their cellular doublings after day 20-50, depending on the *hTERT* knockout clone, and the halt in cellular proliferation may be explained by the shortening of telomeres. The double knockout experiments were performed with clone 2, which began to demonstrate a plateau in cellular proliferation after 50 days, which is comparable to the time point in which we observe the onset of synthetic lethality here at day 21 (*hTERT* knockout Clone 2 was transduced with guide RNAs targeting each INO80 subunit on day 29, thus day 21 of the experiment was ended at age 55 days, which corresponds to day 24 in the double knockout experiment). After a certain number of telomeres reach a critically short length, cellular growth arrest is triggered, which may be through a p53-dependent manner. Thus, the observed synthetic lethality may require the existence of short telomeres. In order to determine whether this proposed mechanism is truly the case, in the future it would be necessary to analyze the length of telomeres and whether these lengths correlate with the previously observed synthetic lethal phenotype.

If short telomeres are required for the onset of synthetic lethality, this demonstrates that the mechanism contributing to enhanced rates of growth arrest with the addition of the loss of the INO80 complex requires growth arrest to already have begun due to short telomeres. When focusing on the hypothesis that INO80 functions as a repressor of *CDKN1A* transcription, p21 expression induced by short telomeres may be required to see an additive effect with p21 expression induced by the loss of the human INO80 complex.

4.3 P53 target expression is altered after stimulation chemically (nutlin-3a or doxorubicin) or by short telomeres, and the phenotype is enhanced after the deletion of some subunits of the human INO80 complex

Furthermore, there are a variety of possible links between chromatin remodeling and telomere maintenance that could explain the observed synthetic lethality. We hypothesized that the human INO80 complex is functioning as a repressor of *CDKN1A* transcription. After cells are deleted for the gene encoding telomerase, an increase in p21 expression should occur, which results in an additive increase in p21 expression with the loss of INO80. Cells would experience and additive reduction in relative fitness after the loss of both components. Thus, we set out to determine whether there are changes in p53 target expression after the manipulation of either the INO80 complex or telomerase chemically or genetically.

Primarily, the deletion of *hTERT* promotes the upregulation of *CDKN1A*, *BAX* and *MDM2* expression. In addition, chemical stimulation of p53 by nutlin-3a treatment for 6 days or 4 hours increases *CDKN1A* expression, and this phenotype is enhanced after the deletion of *hTERT*. Nutlin-3a treatment for 6 days or 4 hours also increases *BAX* expression but this phenotype is not enhanced by the deletion of *hTERT*. After 6 days of nutlin-3a treatment, *MDM2* expression is only increased after the deletion of *hTERT*, however, after 4 hours of nutlin-3a treatment, *MDM2* expression is increased even without the deletion of *hTERT*.

The loss of telomerase and further shortening of telomeres has been shown to activate a p53 response leading to the activation of p21 and growth arrest (Chin *et al*., 1999, Herbig *et al*., 2004). Thus, it is expected that the downstream effectors of p53 should increase their expression levels in response to the loss of telomerase. Also, the p53 inhibitor, *MDM2* expression is regulated through a feedback loop with p53, and thus, after the stimulation of p53 activation, *MDM2* expression is increased (Barak *et al*., 1993, Wu *et al*., 1993). Additionally, if the expression of p53 pathway components (*CDKN1A*, *BAX* and *MDM2*) is altered after treatment with nutlin-3a, and is enhanced with the deletion of *hTERT*, these two p53 stimuli may work in an additive manner to increase p53 stimulus and pathway activation. If these transcriptional changes are only observed after 4 hours of nutlin-3a treatment, and not observed after 6 days of nutlin-3a treatment, it may be possible that accurate transcriptional changes caused by the compound are short-term, and after cell doublings these changes are somehow mitigated through

adaptation or other downstream responses. Overall, the loss of telomerase increases expression levels of p53 effectors, and this phenotype is enhanced by treatment with the p53 stabilizer, nutlin-3a.

After the deletion of *hTERT* in addition to treatment with the UCHL5 inhibitor NSC-687852 for 6 days, *BAX* expression was observed to increase slightly, but not significantly. However, after 6 days of treatment with another UCHL5 inhibitor, WP-1130, no changes were observed in p53 target expression levels. In cells deleted for the human INO80 complex subunit *NFRKB* and treated with the p53 stabilizer nutlin-3a for 4 hours, significant increases in *CDKN1A* and *MDM2* expression were seen. In cells deleted for another subunit of the human INO80 complex, *UCHL5*, and after treatment with nutlin-3a for 4 hours, significant increases in *MDM2* expression were observed. Overall, p53 target expression levels were altered after the deletion of either *UCHL5* or *NFRKB* in a nutlin-3a-dependent manner.

More changes in the transcription levels of p53 effectors were observed after p53 stabilization by nutlin-3a treatment rather than *hTERT* loss. Thus, the additive effects of each of these routes of p53 stabilization and the loss of certain INO80 complex subunits may be more apparent with INO80 knockout rather than chemical inhibition. Even though the chemical inhibitors of UCHL5 that were used also demonstrated a synthetic lethal phenotype with *hTERT* loss, this may be due to off target effects of the chemical inhibitors. Also, the additivity may be more apparent after 4 hours rather than 6 days of chemical inhibition due to compensatory mechanisms occurring over cell doublings in response to the presence of chemical inhibitors. A better time period to determine transcriptional changes may be 4 hours rather than 6 days. Alterations to p53 target transcription levels after the stimulation of p53 by either nutlin-3a or the loss of *hTERT*, and the enhanced phenotype observed after the deletion of *NFRKB* or *UCHL5*, may occur due to the human INO80 complex's role in repressing *CDKN1A* transcription. With the loss of critical subunits of the INO80 complex, including *NFRKB* and *UCHL5*, the complex cannot function as a repressor of *CDKN1A* transcription. Thus, p21 expression increases, which may affect the transcription levels of *BAX* and *MDM2* in a feedback manner. This increase in expression of p53 effectors may be additive to the increase in p21 expression observed after the loss of *hTERT* or after nutlin-3a treatment. Overall, the p21 expression increase is enhanced and cellular growth arrest occurs at a faster rate in the population.

Previously, Cao *et al*., showed that the loss of the human INO80 complex leads to an increase in *CDKN1A* expression (Cao *et al*., 2015). The complex is suggested to function as a repressor of the transcription of *CDKN1A* in HeLa cells (Cao *et al*., 2015). If this is the case in NALM-6 cells, we would expect to observe an increase in basal p53 target expression levels, specifically *CDKN1A* expression levels after *UCHL5* or *NFRKB* knockout. However, the above results do not show basal expression level alterations. This may be due to lower levels of TP53 expression and p53 targets in NALM-6 cells, thus requiring nutlin-3a for p53 stabilization to see p53 target expression levels change in an INO80 dependent manner. Additionally, MDM2, the E3 ligase targeting p53 for proteasomal degradation, may be more highly expressed or active in NALM-6 cells, thus maintaining low levels of p53 in NALM-6 cells. Overall, we may not be able to see basal changes in p53 target expression levels after the deletion of *UCHL5* or *NFRKB* alone, unless p53 is forced to be stabilized nutlin-3a.

4.4 Synthetic lethality is observed after the deletion of some subunits of the human INO80 complex and p53 stabilization chemically by nutlin-3a or doxorubicin

If the human INO80 complex functions as a repressor of *CDKN1A* transcription, p53 stimulation should increase p53 target expression in addition to the increase already proposed after INO80 subunit deletion. We then set out to determine whether the deletion of INO80 sensitizes cells to p53 stabilizing compounds (e.g. nutlin-3a).

The IC50 value for the p53 indirect stabilizer doxorubicin was lowered after NALM-6 cells were deleted for the human INO80 complex subunit *NFRKB*. In addition, the IC50 value for the p53 stabilizer nutlin-3a was lowered after NALM-6 cells were deleted for the human INO80 complex subunit *UCHL5*. Furthermore, the relative fitness values of cells deleted for either *UCHL5* or *NFRKB* were reduced after treatment of the p53 stabilizers doxorubicin or nutlin-3a for 12 days. One guide RNA for *UCHL5*, I25, did not demonstrate these results, and previous experiments suggest cells transduced with this guide do not represent true knockouts (data not shown). Three other guides used to target *UCHL5* demonstrated synthetic lethality with BIBR1532 treatment, but I25 did not exhibit such synthetic lethality. Thus, each experiment must be repeated with more guides targeting *UCHL5*.

If the IC50 values for each of the p53 stabilizer compounds were lowered in cells deleted for certain subunits of the human INO80 complex, the cells may be more sensitive to perturbations in the p53 pathway. These sensitivities were also replicated but analyzed in terms of proliferation. Overall, cells deleted for certain subunits of the human INO80 complex are more sensitive to the p53 stabilizers nutlin-3a or doxorubicin by requiring a smaller concentration to see growth arrest compared to DMSO, and by limiting proliferation over time compared to non-targeting control knockout cell lines. These observed sensitivities may suggest that the loss of some subunits of the INO80 complex, *UCHL5* and *NFRKB*, are synthetic lethal with p53 stabilizer compounds. This result is comparable to the sensitivity observed to the loss of *hTERT*, and thus p53 stabilization, in cells deleted for certain subunits of the human INO80 complex, including *UCHL5* and *NFRKB*. It may be necessary to have p53 stabilization exogenously or through the loss of *hTERT*, in order to reveal the full extent of the role of INO80.

4.5 Future Directions and Implications

This work provides evidence that after the loss of *hTERT*, known to activate p53 when telomeres become eroded, or by treatment with the p53 chemical stabilizers nutlin-3a or doxorubicin, NALM-6 cells deleted for certain subunits of the human INO80 complex underwent cellular growth arrest at a faster rate than wildtype NALM-6 cells. It is possible that the INO80 complex functions to repress p53 signaling at the *CDKN1A* transcriptional locus in response to the loss of *hTERT*, but the above results suggest a more general repression of p53 signaling, which may occur at other places in the p53 pathway. In order to better understand the mechanism behind the observed synthetic lethality, the following experiments could be performed. In order to determine whether the transcriptional changes in the p53 effectors are not due to off-target effects by compound treatment, it would be worthwhile to generate a double knockout clonal cell line that is deleted for both *hTERT* and each subunit of the human INO80 complex individually, and to then analyze proliferation and alterations to p53 effector transcription levels. It is expected that the double knockout would show increased levels of *CDKN1A*, *BAX* and *MDM2* transcription. In addition, it would be important to grow clonal cells lines that are deleted in each subunit of the human INO80 complex, and to replicate each of the above experiments, as it is necessary to determine whether the subunits that demonstrate

synthetic lethality are the only subunits that demonstrate alterations in p53 target expression levels. Moreover, if the human INO80 complex acts to repress the transcription of *CDKN1A* in a p53 dependent manner, chromatin immunoprecipitation (ChIP) could be performed to view the complex at the promoter regions of *CDKN1A*. It would be interesting to look at the promoter regions of other p53 targets as well. Finally, after removing p53 from the cell, one would predict that all observed phenotypes should be rescued.

This work demonstrates a novel synthetic lethal relationship that could, in principle, be harnessed for therapeutic purposes. Synthetic lethality is gaining more notice as a potential therapeutic approach, as new sensitivities can be targeted for the removal of specific types of cells. For example, a cell may have a specific mutation leading the cell to demonstrate genomic instability and sensitivity to another compound. In this way, if one utilizes a targeted compound or inhibitor, only the cells with that specific mutation will undergo growth arrest. Telomerase inhibitors have proven to be beneficial for cancer cell therapeutics, as telomerase is upregulated in most cancer cells. However, this therapeutic strategy is inefficient due to the time required for telomeres to shorten. Thus, if a synthetic lethal relationship could be identified that occurred earlier after the loss of telomerase, the cancer cells may undergo growth arrest without the required lag period. In conclusion, this work suggests that if cells are inhibited for the function of both telomerase and the INO80 complex, cellular growth arrest can be accelerated. This synthetic lethal relationship may be harnessed to develop new and effective combinatorial therapeutics in cancer.

Previously harnessed synthetic lethal relationships in the clinic include PARP1/BRCA1 as mentioned above. Many other possibilities have been examined and may be specific to cancer cells if discovered in a tumour-specific environment or genetic background (reviewed in O'Neil *et al*., 2017). Conditional synthetic lethality can allow for the specificity of treatment to be enhanced towards cancer cells. For example, the synthetic lethal relationship could be dependent on a hypoxic environment, a certain cancer-specific mutation or replicative stress (reviewed in O'Neil *et al*., 2017). Overall, targeting synthetic lethal interactions for cancer therapeutics is beneficial due to the limited off-target effects, limited adverse effects as well as the wide span of cancer mutations that can be targeted. In this case, inhibiting the function of telomerase may pose a variety of problems therapeutically, including targeting embryonic stem cells for cell death. Harnessing the synthetic lethal relationship between the loss of telomerase (*hTERT*) and

the human INO80 complex may reduce these off-target effects by reducing the dosage or required treatment time of each inhibitor required to exhibit the same cancer cell death phenotype.

Conclusions

Overall, this study demonstrated a reduction in relative fitness after the genetic or chemical abrogation of the human INO80 complex and telomerase. This synthetic lethal phenotype was observed after 21 days, which is consistent with the lag period required for telomere shortening to occur. Furthermore, alterations in p53 target expression occurred after the chemical stabilization of p53 or p53 induction by induced telomere erosion, which was enhanced after the loss of specific subunits of the human INO80 complex, including *NFRKB* and *UCHL5*. Preliminary data also suggested that p53 activation may be required for the aforementioned synthetic lethal phenotype to be observed. Finally, the loss of the INO80 complex sensitizes cells to p53 stabilizing compounds. Overall, the activation of the p53 pathway is important for reduced cell fitness, and this phenotype is enhanced after the loss of the human INO80 complex.

Bibliography

Abbas, T., & Dutta, A. (2009). P21 in cancer: Intricate networks and multiple activities. *Nature Reviews Cancer*. https://doi.org/10.1038/nrc2657

Affar, E. B., Gay, F., Shi, Y., Liu, H., Huarte, M., Wu, S., … Shi, Y. (2006). Essential Dosage-Dependent Functions of the Transcription Factor Yin Yang 1 in Late Embryonic Development and Cell Cycle Progression. *Molecular and Cellular Biology*, *26*(9), 3565–3581. https://doi.org/10.1128/mcb.26.9.3565-3581.2006

Agarwal, M. L., Agarwal, A., Taylor, W. R., & Stark, G. R. (1995). p53 controls both the G2/M and the G1 cell cycle checkpoints and mediates reversible growth arrest in human fibroblasts. *Proceedings of the National Academy of Sciences of the United States of America*, *92*(18), 8493–8497. https://doi.org/10.1073/pnas.92.18.8493

Allsopp, R. C., Vaziri, H., Patterson, C., Goldstein, S., Younglai, E. V., Futcher, A. B., … Harley, C. B. (1992). Telomere length predicts replicative capacity of human fibroblasts. *Proceedings of the National Academy of Sciences of the United States of America*, *89*(21), 10114–10118. https://doi.org/10.1073/pnas.89.21.10114

Bacchetti, S., & Counter, C. M. (1995). Telomeres and telomerase in human cancer. (Review). *International Journal of Oncology*. https://doi.org/10.3892/ijo.7.3.423

Barak, Y., Juven, T., Haffner, R., & Oren, M. (1993). *MDM2* expression is induced by wild type p53 activity. *The EMBO Journal*, *12*(2), 461–468. https://doi.org/10.1002/j.1460-2075.1993.tb05678.x

Bartek, J., & Lukas, J. (2001). Mammalian G1- and S-phase checkpoints in response to DNA damage. *Current Opinion in Cell Biology*. https://doi.org/10.1016/S0955-0674(00)00280-5

Baumann, P., & Cech, T. R. (2001). Pot1, the putative telomere end-binding protein in fission yeast and humans. *Science*, *292*(5519), 1171–1175. https://doi.org/10.1126/science.1060036

Bertomeu, T., Coulombe-Huntington, J., Chatr-aryamontri, A., Bourdages, K. G., Coyaud, E., Raught, B., … Tyers, M. (2017). A High-Resolution Genome-Wide CRISPR/Cas9 Viability Screen Reveals Structural Features and Contextual Diversity of the Human Cell-Essential Proteome. *Molecular and Cellular Biology*, *38*(1). https://doi.org/10.1128/mcb.00302-17

Bilaud, T., Brun, C., Ancelin, K., Koering, C. E., Laroche, T., & Gilson, E. (1997). Telomeric localization of TRF2, a novel human telobox protein. *Nature Genetics*. https://doi.org/10.1038/ng1097-236

Blackburn, E. H. (1984). Telomeres: Do the ends justify the means? *Cell*. https://doi.org/10.1016/0092-8674(84)90295-2

Blasco, M. A., Lee, H. W., Hande, M. P., Samper, E., Lansdorp, P. M., DePinho, R. A., & Greider, C. W. (1997). Telomere shortening and tumour formation by mouse cells lacking telomerase RNA. *Cell*, *91*(1), 25–34. https://doi.org/10.1016/S0092-8674(01)80006-4

Bodnar, A. G., Ouellette, M., Frolkis, M., Holt, S. E., Chiu, C. P., Morin, G. B., … Wright, W. E. (1998). Extension of life-span by introduction of telomerase into normal human cells. *Science*, *279*(5349), 349–352. https://doi.org/10.1126/science.279.5349.349

Brahma, S., Udugama, M. I., Kim, J., Hada, A., Bhardwaj, S. K., Hailu, S. G., … Bartholomew, B. (2017). INO80 exchanges H2A.Z for H2A by translocating on DNA proximal to histone dimers. *Nature Communications*, *8*. https://doi.org/10.1038/ncomms15616

Bridges, C. B. (1922). The Origin of Variations in Sexual and Sex-Limited Characters. *The American Naturalist*, *56*(642), 51–63. https://doi.org/10.1086/279847

Broccoli, D., Smogorzewska, A., Chong, L., & de Lange, T. (1997). Human telomeres contain two distinct Myb-related proteins, TRF1 and TRF2. *Nature Genetics*. https://doi.org/10.1038/ng1097-231

Broccoli, D., Young, J. W., & De Lange, T. (1995). Telomerase activity in normal and malignant hematopoietic cells. *Proceedings of the National Academy of Sciences of the United States of America*, *92*(20), 9082–9086. https://doi.org/10.1073/pnas.92.20.9082

Brugarolas, J., Chandrasekaran, C., Gordon, J. I., Beach, D., Jacks, T., & Hannon, G. J. (1995). Radiation-induced cell cycle arrest compromised by p21 deficiency. *Nature*. https://doi.org/10.1038/377552a0

Bryan, C., Rice, C., Hoffman, H., Harkisheimer, M., Sweeney, M., & Skordalakes, E. (2015). Structural basis of telomerase inhibition by the highly specific BIBR1532. *Structure*, *23*(10), 1934–1942. https://doi.org/10.1016/j.str.2015.08.006

Bryan, T. M., Englezou, A., Gupta, J., Bacchetti, S., & Reddel, R. R. (1995). Telomere elongation in immortal human cells without detectable telomerase activity. *The EMBO Journal*, *14*(17), 4240–4248. https://doi.org/10.1002/j.1460-2075.1995.tb00098.x

Bryan, T. M., & Reddel, R. R. (1997). Telomere dynamics and telomerase activity in in vitro immortalised human cells. *European Journal of Cancer Part A*, *33*(5), 767–773. https://doi.org/10.1016/S0959-8049(97)00065-8

Cao, L., Ding, J., Dong, L., Zhao, J., Su, J., Wang, L., … Cai, Y. (2015). Negative regulation of p21Waf1/Cip1 by human INO80 chromatin remodeling complex is implicated in cell cycle phase G2/M arrest and abnormal chromosome stability. *PLoS ONE*, *10*(9). https://doi.org/10.1371/journal.pone.0137411

Chen, L., Cai, Y., Jin, G., Florens, L., Swanson, S. K., Washburn, M. P., … Conaway, R. C. (2011). Subunit organization of the human INO80 chromatin remodeling complex: An evolutionarily conserved core complex catalyzes ATP-dependent nucleosome remodeling. *Journal of Biological Chemistry*, *286*(13), 11283–11289. https://doi.org/10.1074/jbc.M111.222505

Cheung, H. W., Cowley, G. S., Weir, B. A., Boehm, J. S., Rusin, S., Scott, J. A., … Hahn, W. C. (2011). Systematic investigation of genetic vulnerabilities across cancer cell lines reveals lineage-specific dependencies in ovarian cancer. *Proceedings of the National Academy of Sciences of the United States of America*, *108*(30), 12372–12377. https://doi.org/10.1073/pnas.1109363108

Chin, L., Artandi, S. E., Shen, Q., Tam, A., Lee, S. L., Gottlieb, G. J., … DePinho, R. A. (1999). p53 deficiency rescues the adverse effects of telomere loss and cooperates with telomere dysfunction to accelerate carcinogenesis. *Cell*, *97*(4), 527–538. https://doi.org/10.1016/S0092-8674(00)80762-X

Chong, L., Van Steensel, B., Broccoli, D., Erdjument-Bromage, H., Hanish, J., Tempst, P., & De Lange, T. (1995). A human telomeric protein. *Science*, *270*(5242), 1663–1667. https://doi.org/10.1126/science.270.5242.1663

Collins, K., & Greider, C. W. (1995). Utilization of ribonucleotides and RNA primers by Tetrahymena telomerase. *The EMBO Journal*, *14*(21), 5422–5432. https://doi.org/10.1002/j.1460-2075.1995.tb00226.x

Damalas, A., Kahan, S., Shtutman, M., Ben-Ze'ev, A., & Oren, M. (2001). Deregulated β-catenin induces a p53- and ARF-dependent growth arrest and cooperates with Ras in transformation. *EMBO Journal*, *20*(17), 4912–4922. https://doi.org/10.1093/emboj/20.17.4912

Damm, K., Hemmann, U., Garin-Chesa, P., Hauel, N., Kauffmann, I., Priepke, H., … Schnapp, A. (2001). A highly selective telomerase inhibitor limiting human cancer cell proliferation. *EMBO Journal*, *20*(24), 6958–6968. https://doi.org/10.1093/emboj/20.24.6958

De Lange, T. (2005). Shelterin: The protein complex that shapes and safeguards human telomeres. *Genes and Development*. https://doi.org/10.1101/gad.1346005

Deng, C., Zhang, P., Wade Harper, J., Elledge, S. J., & Leder, P. (1995). Mice Lacking p21 CIP1/WAF1 undergo normal development, but are defective in G1 checkpoint control. *Cell*, *82*(4), 675–684. https://doi.org/10.1016/0092-8674(95)90039-X

Dimri, G. P., Itahana, K., Acosta, M., & Campisi, J. (2000). Regulation of a Senescence Checkpoint Response by the E2F1 Transcription Factor and p14ARF Tumour Suppressor. *Molecular and Cellular Biology*, *20*(1), 273–285. https://doi.org/10.1128/mcb.20.1.273-285.2000

Dobzhansky T. (1946). Genetics of natural populations; recombination and variability in populations of Drosophila pseudoobscura. *Genetics*, *31*, 269–290.

Ebbert, R., Birkmann, A., & Schüller, H. J. (1999). The product of the SNF2/SWI2 paralogue INO80 of Saccharomyces cerevisiae required for efficient expression of various yeast structural genes is part of a high-molecular-weight protein complex. *Molecular Microbiology*, *32*(4), 741–751. https://doi.org/10.1046/j.1365-2958.1999.01390.x

El-Daly, H., Kull, M., Zimmermann, S., Pantic, M., Waller, C. F., & Martens, U. M. (2005). Selective cytotoxicity and telomere damage in leukemia cells using the telomerase inhibitor BIBR1532. *Blood*, *105*(4), 1742–1749. https://doi.org/10.1182/blood-2003-12-4322

El-Deiry, W. S., Tokino, T., Velculescu, V. E., Levy, D. B., Parsons, R., Trent, J. M., … Vogelstein, B. (1993). WAF1, a potential mediator of p53 tumour suppression. *Cell*, *75*(4), 817–825. https://doi.org/10.1016/0092-8674(93)90500-P

Farmer, H., McCabe, H., Lord, C. J., Tutt, A. H. J., Johnson, D. A., Richardson, T. B., … Ashworth, A. (2005). Targeting the DNA repair defect in BRCA mutant cells as a therapeutic strategy. *Nature*, *434*(7035), 917–921. https://doi.org/10.1038/nature03445

Feng, J., Funk, W. D., Wang, S. S., Weinrich, S. L., Avilion, A. A., Chiu, C. P., … Villeponteau, B. (1995). The RNA component of human telomerase. *Science*, *269*(5228), 1236–1241. https://doi.org/10.1126/science.7544491

Greider, C. W. (1991). Telomerase is processive. *Molecular and Cellular Biology*, *11*(9), 4572–4580. https://doi.org/10.1128/mcb.11.9.4572

Greider, C. W., & Blackburn, E. H. (1985). Identification of a specific telomere terminal transferase activity in tetrahymena extracts. *Cell*, *43*(2 PART 1), 405–413. https://doi.org/10.1016/0092-8674(85)90170-9

Griffith, J. D., Comeau, L., Rosenfield, S., Stansel, R. M., Bianchi, A., Moss, H., & De Lange, T. (1999). Mammalian telomeres end in a large duplex loop. *Cell*, *97*(4), 503–514. https://doi.org/10.1016/S0092-8674(00)80760-6

Gupta, R., Somyajit, K., Narita, T., Maskey, E., Stanlie, A., Kremer, M., … Choudhary, C. (2018). DNA Repair Network Analysis Reveals Shieldin as a Key Regulator of NHEJ and PARP Inhibitor Sensitivity. *Cell*, *173*(4), 972–988.e23. https://doi.org/10.1016/j.cell.2018.03.050

Hahn, W. C., Stewart, S. A., Brooks, M. W., York, S. G., Eaton, E., Kurachi, A., … Weinberg, R. A. (1999). Inhibition of telomerase limits the growth of human cancer cells. *Nature Medicine*, *5*(10), 1164–1170. https://doi.org/10.1038/13495

Hall, J. M., Lee, M. K., Newman, B., Morrow, J. E., Anderson, L. A., Huey, B., & King, M. C. (1990). Linkage of early-onset familial breast cancer to chromosome 17q21. *Science*, *250*(4988), 1684–1689. https://doi.org/10.1126/science.2270482

Harley, C. B. (1991). Telomere loss: mitotic clock or genetic time bomb? *Mutation Research DNAging*, *256*(2–6), 271–282. https://doi.org/10.1016/0921-8734(91)90018-7

Harrington, L., Zhou, W., McPhail, T., Oulton, R., Yeung, D. S. K., Mar, V., … Robinson, M. O. (1997). Human telomerase contains evolutionarily conserved catalytic and structural subunits. *Genes and Development*, *11*(23), 3109–3115. https://doi.org/10.1101/gad.11.23.3109

Hart, T., Chandrashekhar, M., Aregger, M., Steinhart, Z., Brown, K. R., MacLeod, G., … Moffat, J. (2015). High-Resolution CRISPR Screens Reveal Fitness Genes and Genotype-Specific Cancer Liabilities. *Cell*, *163*(6), 1515–1526. https://doi.org/10.1016/j.cell.2015.11.015

Hartwell, L. H., Szankasi, P., Roberts, C. J., Murray, A. W., & Friend, S. H. (1997). Integrating genetic approaches into the discovery of anticancer drugs. *Science*. https://doi.org/10.1126/science.278.5340.1064

Hartwell, L. H., & Weinert, T. A. (1989). Checkpoints: Controls that ensure the order of cell cycle events. *Science*, *246*(4930), 629–634. https://doi.org/10.1126/science.2683079

Hayflick, L. (1965). The limited in vitro lifetime of human diploid cell strains. *Experimental Cell Research*, *37*(3), 614–636. https://doi.org/10.1016/0014-4827(65)90211-9

Hayflick, L., & Moorhead, P. S. (1961). The serial cultivation of human diploid cell strains. *Experimental Cell Research*, *25*(3), 585–621. https://doi.org/10.1016/0014-4827(61)90192-6

Heiss, N. S., Knight, S. W., Vulliamy, T. J., Klauck, S. M., Wiemann, S., Mason, P. J., … Dokal, I. (1998). X-linked dyskeratosis congenita is caused by mutations in a highly conserved gene with putative nucleolar functions. *Nature Genetics*, *19*(1), 32–38. https://doi.org/10.1038/ng0598-32

Herbig, U., Jobling, W. A., Chen, B. P. C., Chen, D. J., & Sedivy, J. M. (2004). Telomere shortening triggers senescence of human cells through a pathway involving ATM, p53, and p21CIP1, but not p16INK4a. *Molecular Cell*, *14*(4), 501–513. https://doi.org/10.1016/S1097-2765(04)00256-4

Hu, Y., Tang, H. B., Liu, N. N., Tong, X. J., Dang, W., Duan, Y. M., … Zhou, J. Q. (2013). Telomerase-Null Survivor Screening Identifies Novel Telomere Recombination Regulators. *PLoS Genetics*, *9*(1). https://doi.org/10.1371/journal.pgen.1003208

Jin, J., Cai, Y., Yao, T., Gottschalk, A. J., Florens, L., Swanson, S. K., … Conaway, J. W. (2005). A mammalian chromatin remodeling complex with similarities to the yeast INO80 complex. *Journal of Biological Chemistry*, *280*(50), 41207–41212. https://doi.org/10.1074/jbc.M509128200

John C. Lucchesi. (1968). Synthetic lethality and semi-lethality among functionally related mutants of drosophila melanogaster. *Genetics*, *59*(3), 37–44. https://doi.org/10.2116/analsci.22.627

Kaelin, W. G. (2004). Gleevec: prototype or outlier? *Science's STKE : Signal Transduction Knowledge Environment*. https://doi.org/10.1126/stke.2252004pe12

Kilian, A., Bowtell, D. D. L., Abud, H. E., Hime, G. R., Venter, D. J., Keese, P. K., … Jefferson, R. A. (1997). Isolation of a candidate human telomerase catalytic subunit gene, which reveals complex splicing patterns in different cell types. *Human Molecular Genetics*, *6*(12), 2011–2019. https://doi.org/10.1093/hmg/6.12.2011

Kim, N. W., Piatyszek, M. A., Prowse, K. R., Harley, C. B., West, M. D., Ho, P. L. C., … Shay, J. W. (1994). Specific association of human telomerase activity with immortal cells and cancer. *Science*, *266*(5193), 2011–2015. https://doi.org/10.1126/science.7605428

Kiss, T., Fayet, E., Jády, B. E., Richard, P., & Weber, M. (2006). Biogenesis and intranuclear trafficking of human box C/D and H/ACA RNPs. In *Cold Spring Harbor Symposia on Quantitative Biology* (Vol. 71, pp. 407–417). https://doi.org/10.1101/sqb.2006.71.025

Klopf, E., Paskova, L., Sole, C., Mas, G., Petryshyn, A., Posas, F., … Schuller, C. (2009). Cooperation between the INO80 Complex and Histone Chaperones Determines Adaptation of Stress Gene Transcription in the Yeast Saccharomyces cerevisiae. *Molecular and Cellular Biology*, *29*(18), 4994–5007. https://doi.org/10.1128/mcb.01858-08

Krietenstein, N., Wal, M., Watanabe, S., Park, B., Peterson, C. L., Pugh, B. F., & Korber, P. (2016). Genomic Nucleosome Organization Reconstituted with Pure Proteins. *Cell*, *167*(3), 709–721.e12. https://doi.org/10.1016/j.cell.2016.09.045

Lademann, C. A., Renkawitz, J., Pfander, B., & Jentsch, S. (2017). The INO80 Complex Removes H2A.Z to Promote Presynaptic Filament Formation during Homologous Recombination. *Cell Reports*, *19*(7), 1294–1303. https://doi.org/10.1016/j.celrep.2017.04.051

Lendvay, T. S., Morris, D. K., Sah, J., Balasubramanian, B., & Lundblad, V. (1996). Senescence mutants of Saccharomyces cerevisiae with a defect in telomere replication identify three additional EST genes. *Genetics*, *144*(4), 1399–1412.

Levine, A. J. (1997). p53, the cellular gatekeeper for growth and division. *Cell*. https://doi.org/10.1016/S0092-8674(00)81871-1

Lingner, J., & Cech, T. R. (1996). Purification of telomerase from Euplotes aediculatus: Requirement of a primer 3′ overhang. *Proceedings of the National Academy of Sciences of the United States of America*, *93*(20), 10712–10717. https://doi.org/10.1073/pnas.93.20.10712

Lingner, J., Hughes, T. R., Shevchenko, A., Mann, M., Lundblad, V., & Cech, T. R. (1997). Reverse transcriptase motifs in the catalytic subunit of telomerase. *Science*, *276*(5312), 561–567. https://doi.org/10.1126/science.276.5312.561

Lundblad, V., & Szostak, J. W. (1989). A mutant with a defect in telomere elongation leads to senescence in yeast. *Cell*, *57*(4), 633–643. https://doi.org/10.1016/0092-8674(89)90132-3

McClintock, B. (1941). The Stability of Broken Ends of Chromosomes in Zea Mays. *Genetics*, *26*(2), 234–282. Retrieved from http://www.ncbi.nlm.nih.gov/pubmed/17247004%0Ahttp://www.pubmedcentral.nih.gov/articlerender.fcgi?artid=PMC1209127

Meyerson, M., Counter, C. M., Eaton, E. N., Ellisen, L. W., Steiner, P., Caddle, S. D., … Weinberg, R. A. (1997). hEST2, the putative human telomerase catalytic subunit gene, is up- regulated in tumour cells and during immortalization. *Cell*, *90*(4), 785–795. https://doi.org/10.1016/S0092-8674(00)80538-3

Miki, Y., Swensen, J., Shattuck-eidens, D., Futreal, P. A., Harshman, K., Tavtigian, S., … Skolnick, M. H. (1994). Strong Candidate for the Breast and Ovarian Cancer. *Science*, *266*(October), 66–71. https://doi.org/10.1126/science.7545954

Mitchell, J. R., Cheng, J., & Collins, K. (1999). A Box H/ACA Small Nucleolar RNA-Like Domain at the Human Telomerase RNA 3′ End. *Molecular and Cellular Biology*, *19*(1), 567–576. https://doi.org/10.1128/mcb.19.1.567

Mitchell, J. R., & Collins, K. (2000). Human telomerase activation requires two independent interactions between telomerase RNA and telomerase reverse transcriptase. *Molecular Cell*, *6*(2), 361–371. https://doi.org/10.1016/S1097-2765(00)00036-8

Miyake, Y., Nakamura, M., Nabetani, A., Shimamura, S., Tamura, M., Yonehara, S., … Ishikawa, F. (2009). RPA-like Mammalian Ctc1-Stn1-Ten1 Complex Binds to Single-Stranded DNA and Protects Telomeres Independently of the Pot1 Pathway. *Molecular Cell*, *36*(2), 193–206. https://doi.org/10.1016/j.molcel.2009.08.009

Miyashita, T., Krajewski, S., Krajewska, M., Wang, H. G., Lin, H. K., Liebermann, D. A., … Reed, J. C. (1994). Tumour suppressor p53 is a regulator of bcl-2 and *BAX* gene expression in vitro and in vivo. *Oncogene*, *9*(6), 1799–1805.

Momand, J., Zambetti, G. P., Olson, D. C., George, D., & Levine, A. J. (1992). The mdm-2 oncogene product forms a complex with the p53 protein and inhibits p53-mediated transactivation. *Cell*, *69*(7), 1237–1245. https://doi.org/10.1016/0092-8674(92)90644-R

Morin, G. B. (1989). The human telomere terminal transferase enzyme is a ribonucleoprotein that synthesizes TTAGGG repeats. *Cell*, *59*(3), 521–529. https://doi.org/10.1016/0092-8674(89)90035-4

Muller, H. J. (1941). INDUCED MUTATIONS IN DROSOPHILA. *Cold Spring Harbor Symposia on Quantitative Biology*, *9*(0), 151–167. https://doi.org/10.1101/sqb.1941.009.01.019

Muller, J. H. (1938). The remaking of chromosomes. *The Collectiong Net*, *XIII*(116), 180–195.

N., S., E., Z., & S.Ç., K. (2010). A child with severe form of dyskeratosis congenita and TINF2 mutation of shelterin complex. *Pediatric Blood and Cancer*, *55*(6), 1185–1186. https://doi.org/10.1002/pbc.22624 LK - http://linksource.ebsco.com/linking.aspx?sid=EMBASE&issn=15455009&id=doi:10.1002%2Fpbc.22624&atitle=A+child+with+severe+form+of+dyskeratosis+congenita+and+TINF2+mutation+of+shelterin+complex&stitle=Pediatr.+Blood+Cancer&title=Pediatric+Blood+

and+Cancer&volume=55&issue=6&spage=1185&epage=1186&aulast=Sarper&aufirst=Nazan&auinit=N.&aufull=Sarper+N.&coden=PBCEA&isbn=&pages=1185-1186&date=2010&auinit1=N&auinitm=

Nakamura, T. M., Morin, G. B., Chapman, K. B., Weinrich, S. L., Andrews, W. H., Lingner, J., … Cech, T. R. (1997). Telomerase catalytic subunit homologs from fission yeast and human. *Science*, *277*(5328), 955–959. https://doi.org/10.1126/science.277.5328.955

Nakayama J, Tahara H, Tahara E, Saito M, Ito K, Nakamura H, … Ishikawa F. (1998). Telomerase activation by hTRT in human normal fibroblasts and hepatocellular carcinomas. *Nature Genetics*, *18*(1), 65–68.

Natarajan, S., & McEachern, M. J. (2002). Recombinational Telomere Elongation Promoted by DNA Circles. *Molecular and Cellular Biology*, *22*(13), 4512–4521. https://doi.org/10.1128/mcb.22.13.4512-4521.2002

Neckers, L., & Neckers, K. (2005). Heat-shock protein 90 inhibitors as novel cancer chemotherapeutics - An update. *Expert Opinion on Emerging Drugs*. https://doi.org/10.1517/14728214.10.1.137

Neumann, F. R., Dion, V., Gehlen, L. R., Tsai-Pflugfelder, M., Schmid, R., Taddei, A., & Gasser, S. M. (2012). Targeted INO80 enhances subnuclear chromatin movement and ectopic homologous recombination. *Genes and Development*, *26*(4), 369–383. https://doi.org/10.1101/gad.176156.111

Nigro, J. M., Baker, S. J., Preisinger, A. C., Jessup, J. M., Hosteller, R., Cleary, K., … Vogelstein, B. (1989). Mutations in the p53 gene occur in diverse human tumour types. *Nature*, *342*(6250), 705–708. https://doi.org/10.1038/342705a0

Nip, J., Strom, D. K., Fee, B. E., Zambetti, G., Cleveland, J. L., & Hiebert, S. W. (1997). E2F-1 cooperates with topoisomerase II inhibition and DNA damage to selectively augment p53-independent apoptosis. *Molecular and Cellular Biology*, *17*(3), 1049–1056. https://doi.org/10.1128/mcb.17.3.1049

O'Brien, W., Stenman, G., & Sager, R. (1986). Suppression of tumour growth by senescence in virally transformed human fibroblasts. *Proceedings of the National Academy of Sciences of the United States of America*, *83*(22), 8659–8663. https://doi.org/10.1073/pnas.83.22.8659

Olovnikov, A. M. (1971). [Principle of marginotomy in template synthesis of polynucleotides]. *Doklady Akademii Nauk SSSR*, *201*(6), 1496–1499. Retrieved from http://www.ncbi.nlm.nih.gov/pubmed/5158754

Olovnikov, A. M. (1973). A theory of marginotomy. The incomplete copying of template margin in enzymic synthesis of polynucleotides and biological significance of the phenomenon. *Journal of Theoretical Biology*, *41*(1), 181–190. https://doi.org/10.1016/0022-5193(73)90198-7

O'Neil, N. J., Bailey, M. L., & Hieter, P. (2017). Synthetic lethality and cancer. *Nature Reviews Genetics*. https://doi.org/10.1038/nrg.2017.47

Papamichos-Chronakis, M., Watanabe, S., Rando, O. J., & Peterson, C. L. (2011). Global regulation of H2A.Z localization by the INO80 chromatin-remodeling enzyme is essential for genome integrity. *Cell*, *144*(2), 200–213. https://doi.org/10.1016/j.cell.2010.12.021

Pascolo, E., Wenz, C., Lingner, J., Hauel, N., Priepke, H., Kauffmann, I., … Schnapp, A. (2002). Mechanism of human telomerase inhibition by BIBR1532, a synthetic, non-nucleosidic drug candidate. *Journal of Biological Chemistry*, *277*(18), 15566–15572. https://doi.org/10.1074/jbc.M201266200

Sanjana, N., Shalem, O., & Zhang, F. (2014). Improved vectors and genome-wide libraries for CRISPR screening. *Improved Vectors and Genome-Wide Libraries for CRISPR Screening*, 6726. https://doi.org/10.1101/006726

Serrano, M., Lin, A. W., McCurrach, M. E., Beach, D., & Lowe, S. W. (1997). Oncogenic ras provokes premature cell senescence associated with accumulation of p53 and p16(INK4a). *Cell*, *88*(5), 593–602. https://doi.org/10.1016/S0092-8674(00)81902-9

Shalem, O., Sanjana, N. E., Hartenian, E., Shi, X., Scott, D. A., Mikkelsen, T. S., … Zhang, F. (2014). Genome-scale CRISPR-Cas9 knockout screening in human cells. *Science*, *343*(6166), 84–87. https://doi.org/10.1126/science.1247005

Shalem, O., Sanjana, N. E., Hartenian, E., Shi, X., Scott, D. A., Mikkelsen, T. S., … Zhang, F. (2014). Genome-scale CRISPR-Cas9 knockout screening in human cells. *Science*, *343*(6166), 84–87. https://doi.org/10.1126/science.1247005

Shampay, J., Szostak, J. W., & Blackburn, E. H. (1984). DNA sequences of telomeres maintained in yeast. *Nature*, *310*(5973), 154–157. https://doi.org/10.1038/310154a0

Shay, J. W., & Wright, W. E. (1996). Telomerase activity in human cancer. *Current Opinion in Oncology*. https://doi.org/10.1097/00001622-199601000-00012

Shen, X., Mizuguchi, G., Hamiche, A., & Carl, W. (2000). A chromatin remodelling complex involved in transcription and DNA processing. *Nature*, *406*(6795), 541–544. https://doi.org/10.1038/35020123

Srinivas, N., Rachakonda, S., & Kumar, R. (2020). Telomeres and telomere length: A general overview. *Cancers*. https://doi.org/10.3390/cancers12030558

Stark, C. (2006). BioGRID: a general repository for interaction datasets. *Nucleic Acids Research*, *34*(90001), D535–D539. https://doi.org/10.1093/nar/gkj109

Surovtseva, Y. V., Churikov, D., Boltz, K. A., Song, X., Lamb, J. C., Warrington, R., … Shippen, D. E. (2009). Conserved Telomere Maintenance Component 1 Interacts with STN1 and Maintains Chromosome Ends in Higher Eukaryotes. *Molecular Cell*, *36*(2), 207–218. https://doi.org/10.1016/j.molcel.2009.09.017

Szerlong, H., Hinata, K., Viswanathan, R., Erdjument-Bromage, H., Tempst, P., & Cairns, B. R. (2008). The HSA domain binds nuclear actin-related proteins to regulate chromatin-remodeling ATPases. *Nature Structural and Molecular Biology*, *15*(5), 469–476. https://doi.org/10.1038/nsmb.1403

Tesmer, V. M., Ford, L. P., Holt, S. E., Frank, B. C., Yi, X., Aisner, D. L., … Wright, W. E. (1999). Two Inactive Fragments of the Integral RNA Cooperate To Assemble Active Telomerase with the Human Protein Catalytic Subunit (*hTERT*) In Vitro. *Molecular and Cellular Biology*, *19*(9), 6207–6216. https://doi.org/10.1128/mcb.19.9.6207

Tewey, K. M., Rowe, T. C., Yang, L., Halligan, B. D., & Liu, L. F. (1984). Adriamycin-induced DNA damage mediated by mammalian DNA topoisomerase II. *Science*, *226*(4673), 466–468. https://doi.org/10.1126/science.6093249

Tollervey, D., & Kiss, T. (1997). Function and synthesis of small nucleolar RNAs. *Current Opinion in Cell Biology*, *9*(3), 337–342. https://doi.org/10.1016/S0955-0674(97)80005-1

Toshiyuki, M., & Reed, J. C. (1995). Tumour suppressor p53 is a direct transcriptional activator of the human *BAX* gene. *Cell*, *80*(2), 293–299. https://doi.org/10.1016/0092-8674(95)90412-3

Truett, G., Walker, A., Truett, A., Mynatt, R., Heeger, P., & Warman, M. (2000). Preparation of PCR-quality DNA with hot sodium hydroxide and tris (HOTSHOT). *Biotechniques*, *29*, 52–54. Retrieved from papers://77017560-5261-4832-956a-1a3383a16426/Paper/p673

Udugama, M., Sabri, A., & Bartholomew, B. (2011). The INO80 ATP-Dependent Chromatin Remodeling Complex Is a Nucleosome Spacing Factor. *Molecular and Cellular Biology*, *31*(4), 662–673. https://doi.org/10.1128/mcb.01035-10

Vandesompele, J., De Preter, K., Pattyn, F., Poppe, B., Van Roy, N., De Paepe, A., & Speleman, F. (2002). Accurate normalization of real-time quantitative RT-PCR data by geometric averaging of multiple internal control genes. *Genome Biology*, *3*(7). https://doi.org/10.1186/gb-2002-3-7-research0034

Vassilev, L. T., Vu, B. T., Graves, B., Carvajal, D., Podlaski, F., Filipovic, Z., … Liu, E. A. (2004). In Vivo Activation of the p53 Pathway by Small-Molecule Antagonists of *MDM2*. *Science*, *303*(5659), 844–848. https://doi.org/10.1126/science.1092472

Vaziri, H., & Benchimol, S. (1998). Reconstitution of telomerase activity in normal human cells leads to elongation of telomeres and extended replicative life span. *Current Biology*, *8*(5), 279–282. https://doi.org/10.1016/S0960-9822(98)70109-5

Von Zglinicki, T. (2002). Oxidative stress shortens telomeres. *Trends in Biochemical Sciences*. https://doi.org/10.1016/S0968-0004(02)02110-2

Vulliamy, T., Marrone, A., Goldman, F., Dearlove, A., Bessler, M., Mason, P. J., & Dokal, I. (2001). The RNA component of telomerase is mutated in autosomal dominant dyskeratosis congenita. *Nature*, *413*(6854), 432–435. https://doi.org/10.1038/35096585

Wang, T., Wei, J. J., Sabatini, D. M., & Lander, E. S. (2014). Genetic Screens in Human Cells Using. *Science (New York, N.Y.)*, *343*(6166), 80–84. https://doi.org/10.1126/science.1246981

Weinert, T. A., & Hartwell, L. H. (1988). The RAD9 Gene Controls the Cell Cycle Saccharomyces cerevisiae. *Science*, *241*, 317–322.

Wooster, R., Bignell, G., Lancaster, J., Swift, S., Seal, S., Mangion, J., … Stratton, M. R. (1995). Identification of the breast cancer susceptibility gene BRCA2. *Nature*, *378*(6559), 789–792. https://doi.org/10.1038/378789a0

Wooster, R., Neuhausen, S. L., Mangion, J., Quirk, Y., Ford, D., Collins, N., … Stratton, M. R. (1994). Localization of a breast cancer susceptibility gene, BRCA2, to chromosome 13q12-13. *Science*, *265*(5181), 2088–2090. https://doi.org/10.1126/science.8091231

Wu, X., Bayle, J. H., Olson, D., & Levine, A. J. (1993). The p53-mdm-2 autoregulatory feedback loop. *Genes and Development*, *7*(7 A), 1126–1132. https://doi.org/10.1101/gad.7.7a.1126

Xiong, Y., Hannon, G. J., Zhang, H., Casso, D., Kobayashi, R., & Beach, D. (1993). P21 is a universal inhibitor of cyclin kinases. *Nature*, *366*(6456), 701–704. https://doi.org/10.1038/366701a0

Yao, T., Song, L., Jin, J., Cai, Y., Takahashi, H., Swanson, S. K., … Conaway, J. W. (2008). Distinct Modes of Regulation of the Uch37 Deubiquitinating Enzyme in the Proteasome and in the Ino80 Chromatin-Remodeling Complex. *Molecular Cell*, *31*(6), 909–917. https://doi.org/10.1016/j.molcel.2008.08.027

Yu, E. Y., Steinberg-Neifach, O., Dandjinou, A. T., Kang, F., Morrison, A. J., Shen, X., & Lue, N. F. (2007). Regulation of Telomere Structure and Functions by Subunits of the INO80 Chromatin Remodeling Complex. *Molecular and Cellular Biology*, *27*(16), 5639–5649. https://doi.org/10.1128/mcb.00418-07

Zhang, S., Liu, X., Bawa-Khalfe, T., Lu, L. S., Lyu, Y. L., Liu, L. F., & Yeh, E. T. H. (2012). Identification of the molecular basis of doxorubicin-induced cardiotoxicity. *Nature Medicine*, *18*(11), 1639–1642. https://doi.org/10.1038/nm.2919

Zhang, X., Mar, V., Zhou, W., Harrington, L., & Robinson, M. O. (1999). Telomere shortening and apoptosis in telomerase-inhibited human tumour cells. *Genes and Development*, *13*(18), 2388–2399. https://doi.org/10.1101/gad.13.18.2388

Zou, Y., Sfeir, A., Gryaznov, S. M., Shay, J. W., & Wright, W. E. (2004). Does a sentinel or a subset of short telomeres determine replicative senescence? *Molecular Biology of the Cell*, *15*(8), 3709–3718. https://doi.org/10.1091/mbc.E04-03-0207

Appendix

Please see attached excel files for supplementary materials.

Supplementary Figure 1 - Oligo Sequences and Functions

Supplementary Figure 2 - Gene Locus PCR Conditions

Supplementary Figure 3 - Guide RNA Indel Efficiency

Supplementary Figure 4 - Genotypes of Knockout Clonal Cell Lines

Also attached are Figure Supplementary Materials for each figure. These data include rough calculations and statistical analysis.